



This is a repository copy of *Evolution of size-dependent flowering in Onopordum illyricum: A quantitative assessment of the role of stochastic selection pressures* .

White Rose Research Online URL for this paper:
<http://eprints.whiterose.ac.uk/1409/>

Article:

Rees, M., Sheppard, A., Briese, D. et al. (1 more author) (1999) Evolution of size-dependent flowering in *Onopordum illyricum*: A quantitative assessment of the role of stochastic selection pressures. *American Naturalist*, 154 (6). pp. 628-651. ISSN 0003-0147

<https://doi.org/10.1086/303268>

Reuse

Unless indicated otherwise, fulltext items are protected by copyright with all rights reserved. The copyright exception in section 29 of the Copyright, Designs and Patents Act 1988 allows the making of a single copy solely for the purpose of non-commercial research or private study within the limits of fair dealing. The publisher or other rights-holder may allow further reproduction and re-use of this version - refer to the White Rose Research Online record for this item. Where records identify the publisher as the copyright holder, users can verify any specific terms of use on the publisher's website.

Takedown

If you consider content in White Rose Research Online to be in breach of UK law, please notify us by emailing eprints@whiterose.ac.uk including the URL of the record and the reason for the withdrawal request.



eprints@whiterose.ac.uk
<https://eprints.whiterose.ac.uk/>

Evolution of Size-Dependent Flowering in *Onopordum illyricum*: A Quantitative Assessment of the Role of Stochastic Selection Pressures

Mark Rees,¹ Andy Sheppard,² David Brieese,² and Marc Mangel^{3,4}

1. Imperial College, Silwood Park, Ascot, Berkshire SL5 7PY, United Kingdom;

2. Commonwealth Scientific and Industrial Research Organisation Division of Entomology, G.P.O. Box 1700, CRC Weed Management Systems, Canberra, Australian Capital Territory 2601, Australia;

3. Department of Environmental Studies, University of California, Santa Cruz, California 95064;

4. Natural Environment Research Council Centre for Population Biology, Silwood Park, Ascot, Berkshire SL5 7PY, United Kingdom

Submitted October 30, 1998; Accepted July 26, 1999

ABSTRACT: We explore the evolution of delayed, size-dependent reproduction in the monocarpic perennial *Onopordum illyricum*, using a range of mathematical models, parameterized with long-term field data. Analysis of the long-term data indicated that mortality, flowering, and growth were age and size dependent. Using mixed models, we estimated the variance about each of these relationships and also individual-specific effects. For the field populations, recruitment was the main density-dependent process, although there were weak effects of local density on growth and mortality. Using parameterized growth models, which assume plants grow along a deterministic trajectory, we predict plants should flower at sizes approximately 50% smaller than observed in the field. We then develop a simple criterion, termed the "1-yr look-ahead criterion," based on equating seed production now with that of next year, allowing for mortality and growth, to determine at what size a plant should flower. This model allows the incorporation of variance about the growth function and individual-specific effects. The model predicts flowering at sizes approximately double that observed, indicating that variance about the growth curve selects for larger sizes at flowering. The 1-yr look-ahead approach is approximate because it ignores growth opportunities more than 1 yr ahead. To assess the accuracy of this approach, we develop a more complicated dynamic state variable model. Both models give similar results indicating the utility of the 1-yr look-ahead criterion. To allow for temporal variation in the model parameters, we used an individual-based model with a genetic algorithm. This gave very accurate prediction of the observed flowering strategies. Sensitivity analysis

of the model suggested that temporal variation in the parameters of the growth equation made waiting to flower more risky, so selected for smaller sizes at flowering. The models clearly indicate the need to incorporate stochastic variation in life-history analyses.

Keywords: individual-based model, genetic algorithm, dynamic state variable model, von Bertalanffy equation, delayed reproduction, monocarpic perennial.

Age at flowering is a critical component of plant fitness, and indeed, it has been argued that fitness is more sensitive to changes in this character than any other (Stearns 1992). As a result of the obvious link with fitness, many theoretical studies have explored the evolution of age and size at maturity (Cole 1954; Charnov and Schaffer 1973; Caswell and Werner 1978; Bell 1980; Young 1981; Klinkhamer and de Jong 1983; Ziolkowski and Kozłowski 1983; Kachi and Hirose 1985; Hirose and Kachi 1986; Roff 1986, 1992; de Jong et al. 1987; Stearns 1992; Charnov 1993; Kawecki 1993; Charlesworth 1994; Kozłowski and Janczur 1994). These studies are designed to identify the selection pressures and trade-offs that operate and so make predictions about the size and age at which organisms should start reproducing; such predictions can be very accurate (Roff 1984; Mangel 1996).

The main benefits of early reproduction are a reduced risk of dying before reproduction and shorter generation time (Cole 1954; Charnov and Schaffer 1973; Roff 1992; Stearns 1992). Other things being equal, reductions in mortality always increase fitness, whereas shorter generation times only increase fitness under certain circumstances and, in particular, may have no effect on fitness in density-regulated populations (Hastings 1978; Bulmer 1985; de Jong et al. 1987; Charnov 1993; Charlesworth 1994). Whether generation time influences fitness depends on where the density dependence acts in the life cycle, making the quantification of density-dependent processes critical when applying life-history theory (Kawecki 1993; Mylius and Diekmann 1995). The costs of early reproduction are reduced fecundity and/or quality of offspring

(Bell 1980; de Jong et al. 1989; Roff 1992; Stearns 1992). In addition to the benefits that accrue through growth and reproduction, delaying reproduction may provide an advantage via bet hedging. This occurs when members of a cohort flower in different years, and there is temporal variation in the quality of the environment for growth and reproduction (Klinkhamer and de Jong 1983; de Jong et al. 1989).

Several previous studies have attempted to assess the selective advantages of delayed reproduction in plants (Caswell and Werner 1978; Lacey et al. 1983; Reinartz 1984; Young 1984, 1990; Kachi and Hirose 1985; Kelly 1985*b*, 1989*b*; de Jong et al. 1989). Most of these studies were designed to show that delayed flowering was adaptive, whereas the studies of Kachi and Hirose (1985), de Jong et al. (1989), and Wesselingh et al. (1997) attempted to predict the optimal size and age at flowering. By maximizing the intrinsic rate of increase, r , Kachi and Hirose predicted that *Oenothera glazioviana* should have a threshold rosette diameter for flowering of about 16 cm, which is close to the median size at flowering observed in the field (14 cm). In addition, they found that size-dependent flowering strategies had higher rates of increase, r , than age-dependent flowering strategies (Kachi and Hirose 1985). For *Cirsium vulgare* and *Cynoglossum officinale*, the predicted optimal minimum weight for flowering was about 5 g, whereas in both species most plants flowered at weights between 1 and 2 g (de Jong et al. 1989). The discrepancy here, in part, reflects the relatively flat relationship between fitness and the minimum weight for flowering, as all minimum flowering weights in the interval 2–10 g had similar fitness; this makes accurate prediction difficult (Mangel and Clark 1988; de Jong et al. 1989). This study used the long-term geometric growth rate as a measure of fitness, which assumes density dependence does not operate and so penalizes late reproduction through decreased population growth. The discrepancy between observed and predicted weights would have been larger had density-dependent processes been included in the model (de Jong et al. 1989). A later study predicted the optimal minimum weight for flowering in *C. officinale*, using a range of different models (Wesselingh et al. 1997). All the models correctly predicted the rank order of flowering sizes in different habitats and gave reasonable quantitative prediction of the range of flowering sizes (Wesselingh et al. 1997).

In this article, we first describe the size- and age-specific demography of *Onopordum illyricum* monitored at two sites over a 6-yr period. The analysis allows the quantification of systematic and stochastic variation in demographic rates with age and size. We then develop a suite of models that predict the size and age at flowering. Using the models, we assess how different types of variability

influence the evolution of flowering strategies. The simplest models predict the size and age at flowering, which maximizes seed production, assuming a constant environment and a deterministic growth trajectory. We compare these predictions with more complex models that include individual-specific heterogeneity in mortality and scatter about the growth curve. These models are of two sorts: the first uses a simple 1-yr look-ahead criterion to determine at what size plants should flower, while the second is based on a dynamic state variable approach (Mangel and Clark 1988). In order to explore the effects of temporal variation in model parameters, we developed individual-based models, which incorporate a simple, genetic algorithm (Sumida et al. 1990). In these models the surface, which describes the relationship between the probability of flowering and plant size and age, was allowed to evolve. These models have the advantage that one does not have to assume a particular measure of fitness. The models indicate both the need to include stochastic variation in life-history analyses and that different types of variability can have qualitatively different effects on the direction of selection. The models also demonstrate that extremely accurate prediction of life-history phenomena is possible, given detailed demographic data.

The Biology of *Onopordum illyricum*

Onopordum species are thistles of rough-grazing pasture distributed largely throughout Mediterranean and semi-arid areas of Eurasia and North Africa. *Onopordum illyricum* is the most widespread species throughout the western Mediterranean region. Like other *Onopordum* species, *O. illyricum* behaves as a biennial or facultative monocarpic perennial both within (Briese et al. 1994) and outside its native range (Groves et al. 1990; Pettit et al. 1996). In Mediterranean pastures, largely dominated by winter annuals, *O. illyricum* lives for several years, and the above-ground parts of nonflowering individuals die back during the summer months. *Onopordum illyricum* is one of 36 thistle species that has become a serious economic weed outside its native range (Sheppard 1996), and in eastern Australia, together with *Onopordum acanthium*, it infests more than a million ha (Briese et al. 1990). The life-history characteristics of *O. illyricum* are similar to other rosette-forming pasture plants. Reproduction only occurs by seed, and the relatively large seeds form a seed bank. Seeds have an initial short-term innate dormancy, following which the majority of seeds acquire induced dormancy, rendering them incapable of immediate germination (Young and Evans 1972; Cavers et al. 1995). This seed bank may persist for at least 20 yr (Goss 1924) but more commonly has a half-life of 2–3 yr (Allan and Holst 1996). Early seed bank decay appears to be the result of germination or mortality

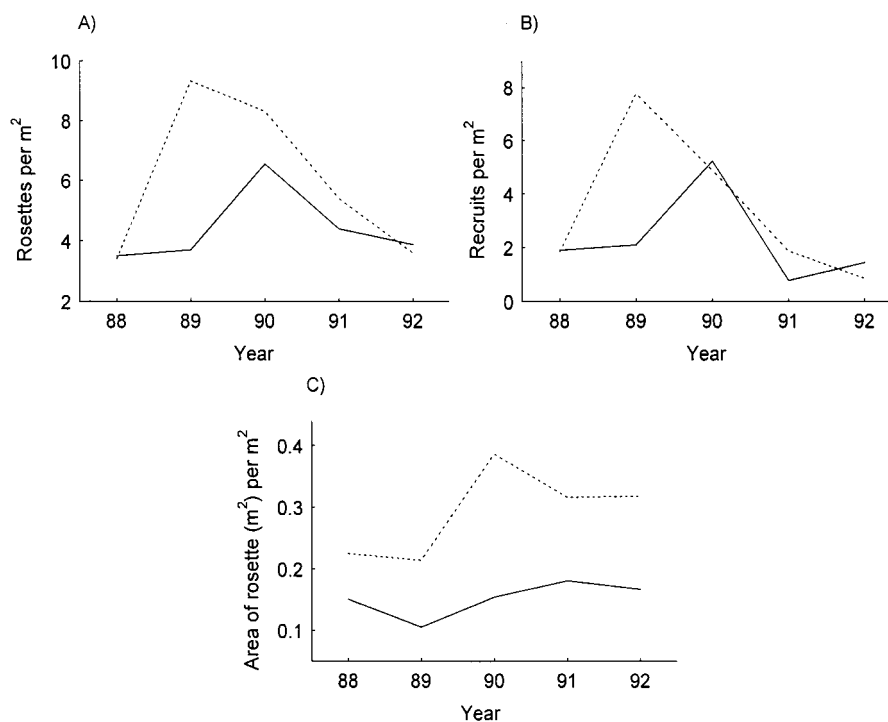


Figure 1: Fluctuations in the density of (A) rosettes, (B) recruits, and (C) total rosette area. *Solid line*, La Crau; *dashed line*, Viols. In the calculation of total rosette area, we assumed that plants were rectangular and that there was no overlap of rosettes. This figure is therefore the maximum rosette area occupied.

from the germinable fraction of the seed bank (Cavers et al. 1995), which suggests that the seed bank decay rate is likely to decrease with time (Rees and Long 1993).

Data Collection

Population data on *Onopordum illyricum* were used from two sites in southern France to parameterize the models. One site was a horse- and cattle-grazed pasture near Viols-en-Laval (Hérault) surrounded by typical garrigue vegetation, while the other was in less productive, sheep-grazed semi-arid steppe habitat in the Plaine du Crau (near St Martin-du-Crau, Bouche-du-Rhône). Both sites contained a relatively dense population of *O. illyricum*, and a core area (40 m × 40 m) was marked out within each population. Twenty 1 × 2-m quadrats were distributed at random within each area, and the position and perpendicular diameters (the longest diameter and its perpendicular diameter in cm) of each plant were recorded on visits in August, November, March, and May. Sampling at the sites took place from August 1987 until August 1992, a period covering the complete life cycle of the first recorded seedling cohort (November 1987).

Between June and August of each year, additional visits

were made to collect and to dissect all capitula produced by plants within the quadrats. Receptacle surface area was measured, and all apparently viable seeds were counted within a few days of collection. Seeds were returned as soon as possible to the quadrat from which they were collected. Returned seeds were shaken from a height of 1.5 m across the general quadrat area in an attempt to simulate natural dispersal. The *O. illyricum* annual minimum seed bank was recorded across each core area from 50 randomly placed 5-cm-diameter × 10-cm-deep soil cores taken just before seed production in June/July in each year. Seeds were washed from the soil cores using sieves, and the extracted seeds were tested for germinability by placing them in moist Petri dishes and then for viability by cutting to examine for a healthy endosperm.

Data Analysis

In most of the analyses, we have focused on the period 1988–1991 inclusive; the 1987 data were excluded because sizes were not recorded and, in the 1992 data, death could not be differentiated from seasonal disappearance. However, if the 1987 or 1992 data provided important information, they were included in the analysis. This, plus the

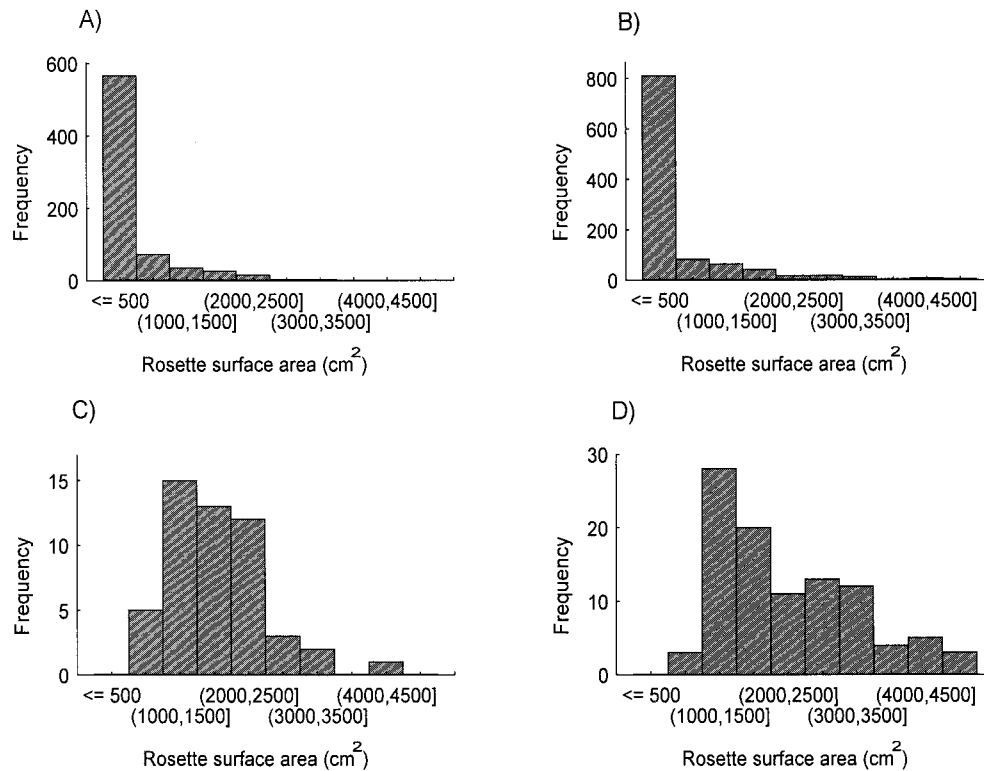


Figure 2: Frequency distributions for maximum rosette area (cm²) at (A) La Crau and (B) Viols for all plants and, for reproductive plants only, at (C) La Crau and (D) Viols.

fact that some plants were not sized in particular years, leads to unavoidable differences in the numbers used in the various analyses.

Selecting a state variable in the construction of the model depends on several factors, including ease of measurement, biological relevance, and predictive ability. In this study, we used the maximum rosette area recorded at the November, March, or May census (most plants had died back by the August census). Preliminary analysis suggested that this variable was the most accurate predictor of plant fate (i.e., death or flowering). It was a better predictor of fate than rosette area at a particular census because it reduced the effects of differences in seasonal phenology between years. However, alternative analyses (not presented) using rosette area at a particular census gave very similar results. In all analyses, where variables were log transformed, natural logarithms were used.

We first provide some simple descriptive analyses of the age and size structure of the populations and how they change through time. The dependence of the probability of dying, the probability of flowering, and the probability of plant size next year on current size and age is then analyzed. Various density-dependent processes are then

quantified before exploring a range of models designed to predict when and at what size plants should flower. A list of the parameters estimated and the variables used in the subsequent models is given in appendix A.

Changes in Numbers, Recruitment, and Area through Time

Total rosette population size fluctuated by a factor of <3 (2.7) at both sites in the period 1988–1992 (see fig. 1); the total area occupied by rosettes fluctuated by a factor of <1.8 over the same period. Neither the number of rosettes nor the total area occupied showed any obvious trends with time. In 1988, there were 140 and 136 plants at La Crau and Viols, respectively, while in 1992 there were 155 plants at La Crau and 144 at Viols. The number of recruits recorded at La Crau fluctuated from a low of 31 in 1991 to a maximum of 208 in 1990 (a 6.7-fold fluctuation), while at Viols the low was 34 in 1992 and the maximum was 311 in 1989 (a 9.1-fold fluctuation).

Age Structure of the Population

Straightforward calculation of the proportion of individuals in each age class or average age is potentially misleading because individuals could only be aged by following them through time. Hence, we allowed for differential recording by calculating the proportion in each age class out of the total number of plants where that age class could have been observed. The resulting distribution was normalized by dividing each term by the total. With this procedure, the average age was 1.9 yr at La Crau and 1.93 yr at Viols. A simple alternative to this procedure is to use only the 1992 data, where ages 1–5 could be observed. With just the 1992 data, the average age at La Crau was 2.36 yr and at Viols 2.63 yr.

Size Structure of the Population

The frequency distribution of maximum rosette area for the total population and those plants that flowered is given in figure 2. In all cases, the distributions were skewed with a long tail to the right. The average maximum rosette area for all plants in the La Crau population is 325 cm²; while for flowering plants it is 1,736 cm². At Viols, the average maximum rosette area is 470 cm² for all plants and 2,208 cm² for flowering plants. The average size of flowering plants, log transformed, varied significantly between sites ($F = 9.1$, $df = 1, 180$, $P < 0.003$).

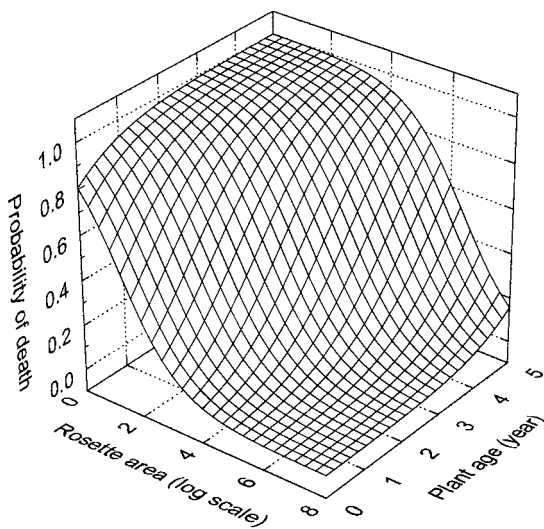


Figure 3: Fitted relationship between the probability of death, plant size, and age for the average mortality model at La Crau. Parameter estimates: $m_0 = 1.42$, $m_1 = -1.08$, $m_2 = 1.09$; at the Viols site, $m_0 = 2.72$. In addition, we have assumed that the individual-specific intercept term, u_i , is equal to 0. This corresponds to the average of the u_i distribution.

Relationships between Mortality, Flowering, Growth, and Plant Size and Age

Mortality. Numerous studies have shown that plant fate can be affected by both size and age (Werner 1975; Baskin and Baskin 1979; van der Meijden and van de Waals-Kooi 1979; Gross 1981; Hirose and Kachi 1982; Gross and Werner 1983; van Baalen and Prins 1983; Reinartz 1984; Klinkhamer and de Jong 1987; Lacey 1988; Kachi 1990; Bullock et al. 1994; Wesselingh et al. 1994; Klinkhamer et al. 1996; Wesselingh and Klinkhamer 1996). The data collected represent a longitudinal study where individuals are followed through time. The statistical analysis of this type of data has developed rapidly in the past few years (see Diggle et al. 1996). In the analysis of mortality and flowering, we used random effects models that allow the regression coefficients to vary from one individual to the next. This variability, estimated by the parameter σ_{δ} , reflects natural heterogeneity due to unmeasured factors. Specifically, for plants, this variability may reflect differences in the local competitive environment, abiotic conditions, levels of herbivore or pathogen attack, or genetic differences between plants. A brief description of these methods, which are not widely used in ecology, is given in appendix B.

We explored two types of model: the first allowed yearly variation in the parameter estimates and is referred to as the “yearly mortality model,” while the second ignored yearly variation and is referred to as the “average mortality model.” Generalized linear models were initially constructed, assuming binomial errors and a logit link function, with a stepwise procedure in S-Plus. This uses an exact calculation of the Akaike Information Criterion (AIC) statistic to determine whether terms should be added or deleted from the model (Becker et al. 1988; Venables and Ripley 1997). This statistic is defined as

$$\text{AIC} = -2 \text{ maximized log likelihood} \\ + 2 \text{ number of parameters,}$$

and so penalizes models that either describe the data poorly or have a large number of parameters. The resulting models were explored further in SABRE, a package designed for fitting regression models incorporating individual-specific heterogeneity (Stott et al. 1996). In all analyses, plant size was log transformed.

In the average mortality model, the main effects of size ($\chi^2_1 = 341.3$, $P < 0.0001$), age ($\chi^2_1 = 25.2$, $P < 0.0001$), and site ($\chi^2_3 = 61.5$, $P < 0.0001$) were all highly significant. There was also evidence of significant individual-specific heterogeneity ($\sigma_{\delta} = 0.82$, $z = 2.2$, $P < 0.02$). None of the interaction terms was statistically significant. The probability of death decreased with plant size but increased with plant age (fig. 3). However, in a model with only age and

site as explanatory variables, the chance of a plant dying decreases with age because larger plants are generally older. Only after size effects have been removed was there an increase in the chance of death with age.

In the yearly mortality model, the most important predictor of mortality was plant size ($\chi_1^2 = 387.3$, $P < 0.0001$); the next most important term was the site by year interaction ($\chi_3^2 = 60.0$, $P < 0.0001$). The effect of age was also highly significant ($\chi_1^2 = 15.2$, $P < 0.0001$). None of the other interaction terms was statistically significant. The fitted relationships for the yearly model are given in figure 4. The individual-specific heterogeneity, σ_ϕ , was highly significant ($\sigma_\phi = 1.3$, $z = 3.02$, $P < 0.002$; for other parameter values, see table 1).

To see how the individual-specific heterogeneity translates into the probability of a plant dying, we computed the probability of death for plants 1, 2, and 3 SDs from the average intercept. It is clear from figure 5 that the estimated levels of individual-specific heterogeneity translate into substantial differences in the risk of death. The average probability of death, for a given age and size, was also calculated with

$$P(\text{death}) = \int \frac{\exp(m_0 + u_i + m_s L + m_a a)}{1 + \exp(m_0 + u_i + m_s L + m_a a)} \times f(u_i) du_i, \quad (1)$$

where m_0 , m_s , and m_a are parameters characterizing size- and age-independent mortality, size-dependent mortality, and age-dependent mortality, respectively, where u_i is an individual-specific term and where $f(u_i)$ is the probability density function of u_i . This differs from the probability of death of a plant with the average intercept because the

probability of death is a nonlinear function of u_i (Stefanski and Carroll 1985; Neuhaus et al. 1991).

Flowering. The same methods for analyzing the probability of mortality were used in the analysis of flowering probability. Plant size, log transformed, was by far the most important predictor of flowering ($\chi_1^2 = 201.9$, $P < 0.0001$), but there were also significant age ($\chi_1^2 = 8.1$, $P < 0.005$) and year ($\chi_3^2 = 8.4$, $P < 0.04$) effects. There were no significant site effects ($\chi_1^2 = 0.1$, $P > 0.1$) or interaction terms. The main effect of year was only marginally significant and accounted for 2% of the deviance and so was not used in any of the subsequent models. The individual-specific heterogeneity, σ_ϕ , was not significant ($\sigma_\phi = 0.52$, $z = 0.39$, $P > 0.1$) and so was dropped from the model. The fitted relationship is given in figure 6.

The relationship between maximum rosette area and fecundity, measured by the area of receptacle matured, is shown in figure 7. In agreement with numerous other studies, there is a linear relationship between fecundity and size on double log axes (Reinartz 1984; de Jong and Klinkhamer 1986; Klinkhamer and de Jong 1987; Rees and Crawley 1989). There were no significant site effects, neither main effect nor interaction terms ($P > 0.1$ in all cases).

Growth. Plant growth was analyzed using linear mixed models in S-Plus (Becker et al. 1988; Venables and Ripley 1997). This approach assumes the vector of observations on each plant is drawn from a multivariate normal distribution. The models allow the incorporation of random individual-specific effects and autocorrelated error terms. In addition, the variance of the response variable may be some simple function of the fitted values. In models with more than one random effect, the estimated individual-

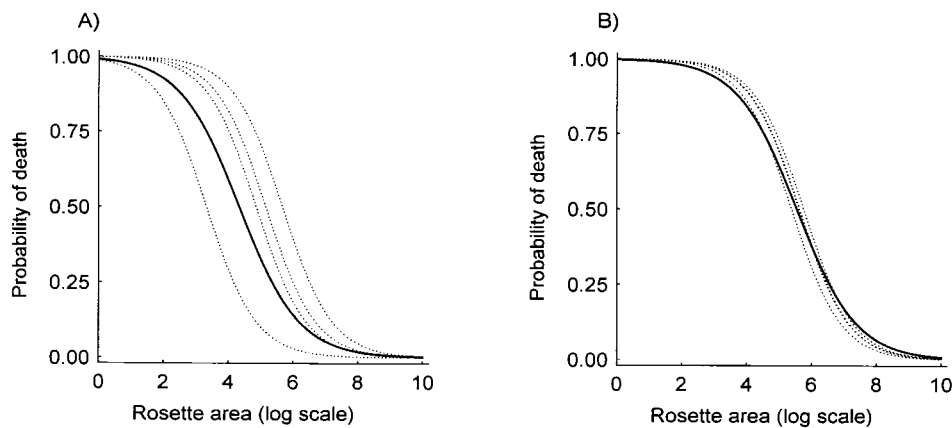


Figure 4: Fitted mortality curves for first-year plants at (A) La Crau and (B) Viols. The solid line is the average model, the dotted lines the yearly model. Parameter values are given in table 1; in addition, we have assumed the individual-specific intercept term, u_i , is equal to 0.

specific effects were highly correlated ($r^2 > 0.99$), suggesting that only one random effect was required in the model. In all the models that follow, we incorporate random individual-specific effects on the intercept; all other model terms are treated as fixed effects. As with the analysis of mortality and flowering, we develop yearly and average models. Preliminary data analysis suggested a linear relationship between log size next year and log size this year, with the variance decreasing with increasing plant size (see fig. 8). We therefore assumed that the variance about the regression line could be modeled as

$$\sigma_g^2 = \varphi \exp(-\alpha \hat{y}), \quad (2)$$

where α and φ are estimated parameters and \hat{y} is the fitted value. This function provided a better fit than other functions, such as power functions or power functions with a constant, using the AIC statistic and diagnostic plots (e.g. standardized residuals vs. fitted values). The residuals from the model may be correlated because of the time series structure of the data. To explore this possibility a model was fitted assuming the covariance matrix was determined by a first-order autoregressive process, AR(1). This assumes the elements of the covariance matrix are given by

$$c_{i,j} = \kappa \rho^{|i-j|}, \quad (3)$$

where κ and ρ are estimated parameters and i and j are two points in time. The inclusion of an AR(1) term did

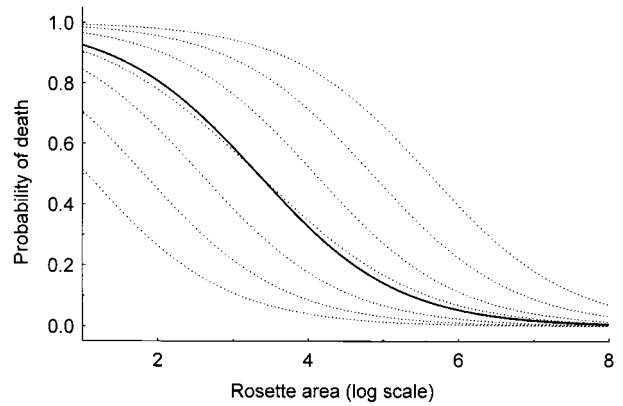


Figure 5: Probability of mortality for a 2-yr-old individual with the mean individual-specific intercept (i.e., $u_i = 0$; middle dotted line) and for individuals $\pm 1, 2, \text{ or } 3 \text{ SD } (\sigma_a)$ from the mean (dotted lines about the central line). Solid line, average mortality for a given size and age, calculated by averaging over the distribution of u_i (see eq. [1]). Note the curve for an individual with the average intercept differs from average mortality, for a given size and age, because the mortality function is nonlinear. For parameter values for the La Crau population, see table 1.

not enter the model significantly ($\chi_1^2 = 2.0, P > 0.1$), so independent, identically distributed errors were used. Significance testing was performed using maximum likelihood estimation but the final model was fitted using restricted maximum likelihood because this reduces the bias

Table 1: Parameter estimates for the average and yearly mortality models

Site	Parameter estimates
Average mortality model:	
La Crau	$\text{logit}(\text{P}(\text{death})) = 1.42 - 1.08L(t) + 1.09a$
Viols	$\text{logit}(\text{P}(\text{death})) = 2.72 - 1.08L(t) + 1.09a$
	$\sigma_a = 0.82$
Yearly mortality model:	
1988:	
La Crau	$\text{logit}(\text{P}(\text{death})) = 2.52 - 1.30L(t) + 1.27a$
Viols	$\text{logit}(\text{P}(\text{death})) = 3.52 - 1.30L(t) + 1.27a$
1989:	
La Crau	$\text{logit}(\text{P}(\text{death})) = 3.57 - 1.30L(t) + 1.27a$
Viols	$\text{logit}(\text{P}(\text{death})) = 3.19 - 1.30L(t) + 1.27a$
1990:	
La Crau	$\text{logit}(\text{P}(\text{death})) = .52 - 1.30L(t) + 1.27a$
Viols	$\text{logit}(\text{P}(\text{death})) = 3.68 - 1.30L(t) + 1.27a$
1991:	
La Crau	$\text{logit}(\text{P}(\text{death})) = 2.90 - 1.30L(t) + 1.27a$
Viols	$\text{logit}(\text{P}(\text{death})) = 3.49 - 1.30L(t) + 1.27a$
	$\sigma_a = 1.30$

Note: In each case $L(t)$ is log size and a is plant age. $\text{Logit}(\text{P}(\text{death}))$ is $\ln\{\text{P}(\text{death})/[1 - \text{P}(\text{death})]\}$, and σ_a is the individual-specific heterogeneity in the intercepts.

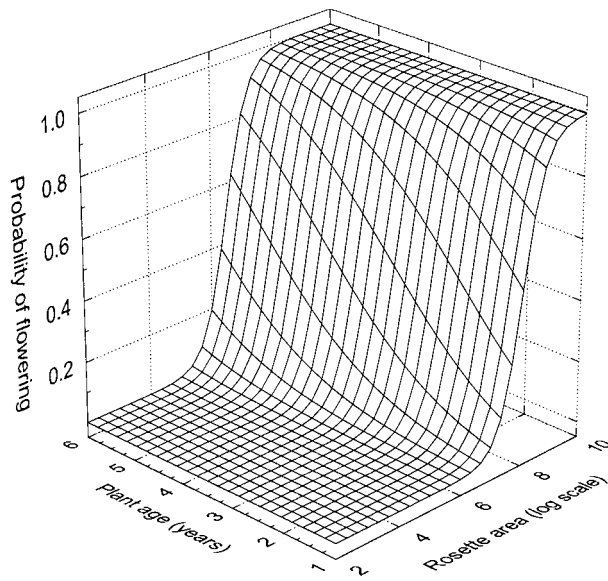


Figure 6: Fitted relationship between the probability of flowering, plant size, and age. Note there were no significant site effects on the probability of flowering. Parameter estimates $\beta_0 = -23.73$ (intercept), $\beta_1 = 2.87$ (size slope), $\beta_2 = 0.85$ (age slope).

in the estimation of the variance components (Diggle et al. 1996; Venables and Ripley 1997).

The average growth model has a significant size by site interaction ($\chi^2_1 = 7.12, P < 0.008$), but age did not enter the model significantly ($z = 1.4, P > 0.08$). The fitted lines are shown in figure 8. In contrast the yearly growth model was much more complicated: there were significant site by size by year ($\chi^2_3 = 38.4, P < 0.0001$) and age by size ($\chi^2_1 = 5.9, P < 0.02$) interactions and also a significant quadratic term in plant size ($\chi^2_1 = 12.3, P < 0.001$). The fitted relationships for 1991, at each of the sites, are shown in figure 9, and the parameter estimates are given in table 2. These surfaces show that plants grow more slowly as they become larger and older.

Detecting Density-Dependent Processes

To test for density-dependent recruitment, we explored the relationship between this year’s seed production and the total number of recruits in the following year, using data from the 20 quadrats at each site (fig. 10). Overall, there is a significant, positive relationship between seed production and subsequent recruitment ($F = 7.08, df = 1, 129, P < 0.01$). However, seed production only accounts for 4% of the variance in the number of recruits, and when those plots where no seed was produced were excluded, the relationship was no longer significant ($F = 1.4, df = 1, 67, P > 0.2$). A constant total number of re-

cruits, over such a wide range of seed production, indicates that the probability that an individual seed recruits decreases with total seed production. A relationship of this form implies that the probability of recruitment, $R(S)$, is proportional to $1/S$:

$$\begin{aligned} \text{Total recruits} &= \text{Constant} = R(S) * S \\ \Rightarrow R(S) &\propto 1/S, \end{aligned} \tag{4}$$

where S is the total seed production.

The presence of a seed bank could potentially obscure any relationship between seed production and recruitment. However, in *Onopordum*, the seed bank is small: over the 4 yr when it was measured at both sites, the maximum density was 190 seeds m^{-2} . It is unlikely that the seed bank would mask any relationship between seed production and recruitment, especially as yearly seed output can be an order of magnitude greater than the seed bank. This uncoupling of recruitment from seed production over such a wide range of seed outputs is an extreme form of density dependence, which is strongly stabilizing. This is probably the result of establishment being limited by the number of suitable microsites. It should be noted that both sites are extremely rocky with thin soils, and recruitment is almost certainly impossible over a high proportion of the area.

The possibility that growth or mortality were dependent on a plant’s local competitive environment was explored by estimating the strength of competition an individual experiences and by regressing its size or the probability of mortality against this (Weiner 1982; Pacala and Silander 1987). The strength of competition was estimated by summing the maximum rosette area of all plants rooted within

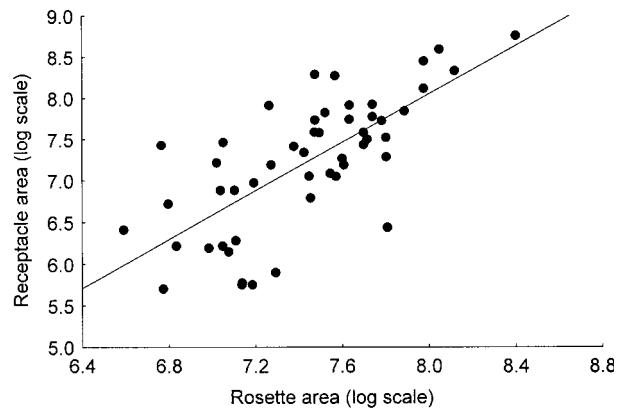


Figure 7: Relationship between rosette area and the area of receptacle matured. Note there were no significant site effects on the relationship between rosette area and the area of receptacle matured. The fitted line is $\log(\text{receptacle area}) = -2.36 + 1.29L, r^2 = 0.57, P < 0.0001$.

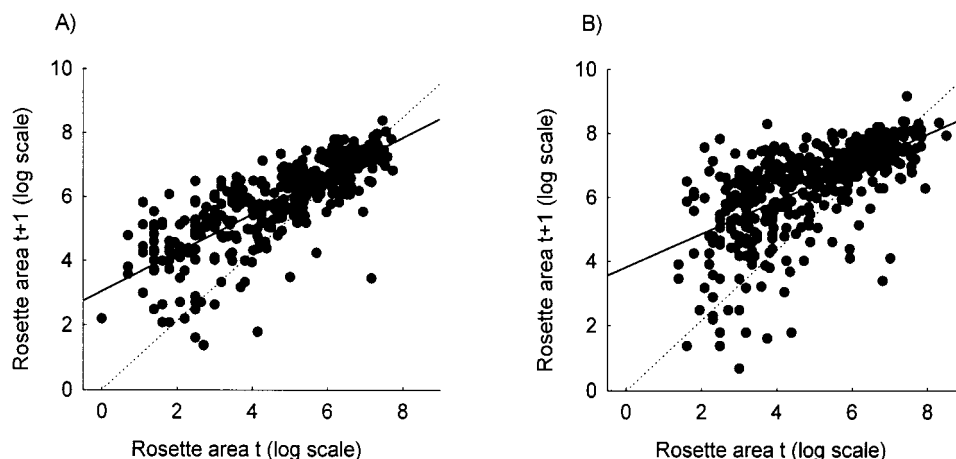


Figure 8: Relationship between rosette area at time t and rosette area at time $t+1$. *A*, La Crau site, fitted relationship is $L(t+1) = 3.05 + 0.6L(t)$. *B*, Viols site, fitted relationship is $L(t+1) = 3.83 + 0.52L(t)$. The variance about the regression line is modeled as $\sigma_s^2 = 45.7 \exp[-0.67\hat{L}(t+1)]$, where $\hat{L}(t+1)$ is the fitted value. The individual-specific heterogeneity in the intercept, σ_i^2 , was estimated at 0.00002. The dotted line is the 1:1 line above which plants increase in size, below which they decrease.

a specified radius around a focal individual. This provides an estimate of the strength of intraspecific competition, but as the vegetative cover at the sites is very sparse, this is likely to be the most important form of competition. Five radii were used in the analysis, namely 10, 20, 30, 40, and 50 cm.

Both growth and mortality were influenced by the local competitive environment (see “Mortality” and “Growth” for descriptions of the statistical methods used). Although in both cases measures of the local competitive environment entered the models significantly ($P < 0.001$), the extra explanatory power of these terms was never $>1.5\%$. This suggests that, over and above the effects of age and size, competition, as measured by the surface area of plants within a certain radius, had little influence on plant growth and mortality. In summary, the main density-dependent process is recruitment, which is almost certainly microsite limited, but there is evidence of weak competition between established plants.

Modeling

We now present a range of models of increasing complexity. The first type of model uses a simple, deterministic growth curve to predict the age and size at flowering. These models ignore all forms of heterogeneity and provide the baseline against which the various refinements, presented later, will be assessed. We then incorporate increasing biological realism by allowing stochastic variation between individuals and in the model parameters.

An Analytical Age-Based Model for Evolutionarily Stable Age and Size at Reproduction

The first model uses a simple age-based function to describe growth in *Onopordum*. The use of growth models to predict the evolutionarily stable size and age at reproduction has an extensive pedigree in the animal literature (Roff 1984, 1986; Stearns 1992; Charnov 1993; Mangel 1996). Specifically, we assume that log size, $L(t)$, at time t can be described by a three-parameter von Bertalanffy equation:

$$L(t) = L_\infty \{1 - \exp[-k(t - t_0)]\}, \quad (5)$$

where L_∞ is the maximum possible size, k is a rate parameter, and t_0 is the hypothetical (negative) age at which size would be 0. The probability an individual survives to time t is a simple exponential function of the form

$$p \exp(-mt), \quad (6)$$

where p is the pulse mortality at the beginning of life and m the instantaneous mortality rate. Finally, we assume that the seed production of an individual of size $L(t)$ is given by

$$\text{seeds} = \exp[A + BL(t)]. \quad (7)$$

Combining these formulas, we can obtain an expression for the net reproductive rate, R_0 , the expected number of offspring produced per individual over their lifespan:

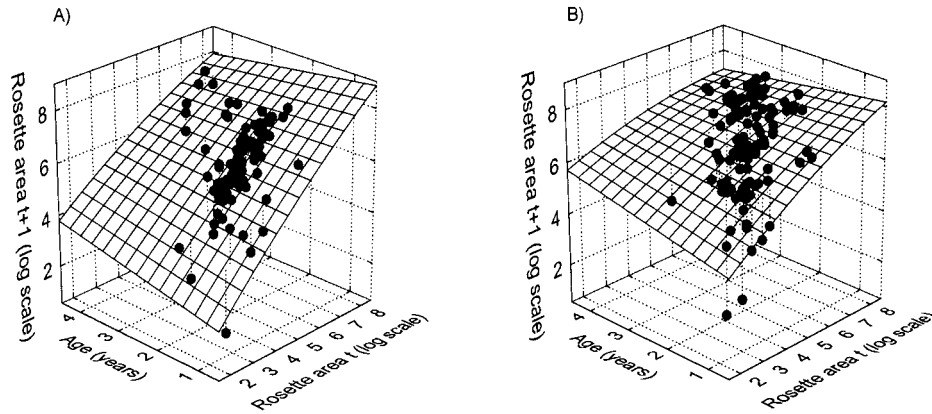


Figure 9: Fitted relationships for the yearly growth model in 1991 at (A) the La Crau site and (B) the Viols site. Parameter values are given in table 2.

$$R_0 = p \exp(-mt) \times \exp [A + B(L_\infty \{1 - \exp[-k(t - t_0)]\})]. \quad (8)$$

The net reproductive rate consists of two components: the first is the probability that an individual survives to age t , and the second is the seed production of a plant of size $L(t)$. We can calculate the evolutionarily stable strategy (ESS) flowering time, \tilde{t} , by solving $\partial R_0 / \partial t = 0$, which gives

$$\tilde{t} = \frac{\ln(BkL_\infty/m)}{k} + t_0. \quad (9)$$

Evolutionary stability occurs if $\partial^2 R_0 / \partial t^2$ evaluated at \tilde{t} is < 0 , which is always true in this case. In calculating the ESS in this way, we are assuming that density dependence acts at the seedling stage (Charnov 1993; Kawecki 1993), which is reasonable for *Onopordum*. Substituting equation (9) into the growth equation (eq. [5]) gives the ESS rosette size for flowering, \tilde{L} ,

$$\tilde{L} = L_\infty - \frac{m}{Bk}. \quad (10)$$

This model can be applied to the *Onopordum* data by estimating the parameters of the growth, survival, and fecundity equations. The von Bertalanffy growth curves were difficult to fit to the data because covariance between the parameters leads to unstable parameter estimates (Ross 1990). Because of this problem, no standard errors could be calculated, and regression diagnostics were used in model selection. The three-parameter von Bertalanffy equation fitted to the combined La Crau and Viols data, assuming common L_∞ and t_0 terms but with k varying

between the sites, provided a good description of the data (see fig. 11). The probability of an individual surviving to age t was estimated using the age-structured data, correcting for the number of individuals flowering. A binomial regression was used to fit the exponential model (eq. [6]); there were no significant site effects for either parameter (p or m , $P > 0.05$ in both cases). The fitted model was

$$P(\text{survival to age } t) = 0.61 \exp(-0.5t). \quad (11)$$

The relationship between fecundity and size is given in figure 7.

Substituting the parameter estimates into equation (10), we predict that the average size at flowering should be $\approx 800 \text{ cm}^2$ at La Crau and $\approx 900 \text{ cm}^2$ at Viols. In both cases, the percentage prediction error is $> 50\%$; the plants actually flowered at sizes approximately double the model predictions. However, plant growth occurs in yearly steps, and so, if these values are interpreted as switch values, below which plants grow and above which they flower, then the observed size at flowering would be larger than the model predictions. Using equation (5), this suggests that plants should flower at $\approx 1,000 \text{ cm}^2$ at both sites. Again, the model predictions are substantially smaller than the values observed in the field. Clearly, this simple model does not accurately predict the patterns of flowering observed in *Onopordum*.

One-Year Look-Ahead Criteria for Flowering and Dynamic State Variable Models

The simple model described above ignores yearly variation in model parameters and individual-specific heterogeneity in mortality rates and assumes growth follows a simple

deterministic trajectory. We now relax the last two assumptions by allowing variation around the growth curve and individual-specific heterogeneity in mortality rates. We use a simple criterion that leads to a switching value L_s ; plants with $L(t) > L_s$ are predicted to reproduce in year t , whereas those with $L(t) < L_s$ are predicted to continue to grow. We compare reproduction given the current size, $L(t)$, with the expected reproduction in the next year, taking growth and survival into account. The switch value will be the size that makes these equal. The switching size satisfies

$$\exp(A + BL_s) = \int \int f(\varepsilon)g(u_i)s(a_g + b_gL_s + \varepsilon, u_i) \times \exp[A + B(a_g + b_gL_s + \varepsilon)]du_id\varepsilon, \quad (12)$$

where ε describes the deviations from the growth curve, u_i is an individual-specific mortality term, $f(\varepsilon)$ and $g(u_i)$ denote the Gaussian probability density functions for ε and u_i , respectively, a_g and b_g are the intercept and slope of the average growth curve (fig. 8), and $s(a_g + b_gL_s + \varepsilon, u_i)$ is the logistic survival function, given by

$$s(a_g + b_gL_s + \varepsilon, u_i) = 1 - \frac{\exp[m_0 + u_i + m_s(a_g + b_gL_s + \varepsilon) + m_a a]}{1 + \exp[m_0 + u_i + m_s(a_g + b_gL_s + \varepsilon) + m_a a]}. \quad (13)$$

The logistic survival term, $s(a_g + b_gL_s + \varepsilon, u_i)$, assumes that growth occurs before mortality in agreement with the seasonal patterns of growth and mortality in *Onopordum*. The term on the left-hand side of equation (12) represents

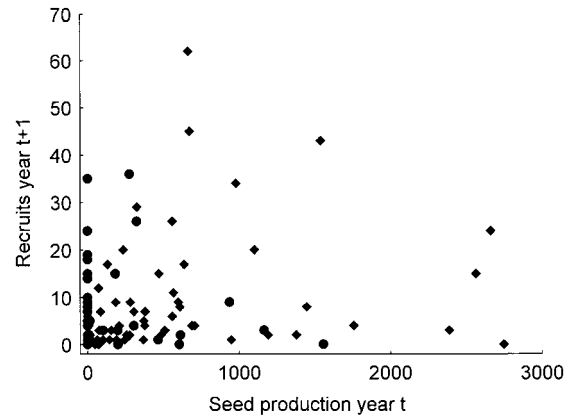


Figure 10: Relationship between this year’s seed production and subsequent recruitment. Circles, the La Crau site; diamonds, Viols.

current reproduction, and the term on the right-hand side represents expected future reproduction, taking growth and survival into account. The integrals were solved numerically using the methods described in Crouch and Spiegelman (1990).

Using the parameter estimates from the average mortality and growth models (fig. 8 and table 1), we can calculate the switch values, L_s , defined by equation (12). Mortality is age and size dependent, so one switch value, L_s , is obtained for each age class (see fig. 12). We then used forward iteration to calculate the average sizes and ages of plants that flower according to these rules (Mangel and Clark 1988). To perform forward iteration, we first generate a recruit from the observed size distribution and then

Table 2: Estimated parameters for the yearly growth model

Year and site	Estimated parameters
1988:	
La Crau	$L(t + 1) = .38 + 1.19L(t) + .48a - .026L(t)^2 - .084L(t)a$
Viols	$L(t + 1) = 3.65 + .69L(t) + .48a - .026L(t)^2 - .084L(t)a$
1989:	
La Crau	$L(t + 1) = 1.82 + .97L(t) + .48a - .026L(t)^2 - .084L(t)a$
Viols	$L(t + 1) = 2.91 + .94L(t) + .48a - .026L(t)^2 - .084L(t)a$
1990:	
La Crau	$L(t + 1) = 2.37 + .94L(t) + .48a - .026L(t)^2 - .084L(t)a$
Viols	$L(t + 1) = .80 + 1.14L(t) + .48a - .026L(t)^2 - .084L(t)a$
1991:	
La Crau	$L(t + 1) = .39 + 1.23L(t) + .48a - .026L(t)^2 - .084L(t)a$
Viols	$L(t + 1) = 2.86 + .86L(t) + .48a - .026L(t)^2 - .084L(t)a$
	$\sigma_g^2 = 38.5 \exp(-.69\hat{L}(t + 1))$
	$\sigma_I^2 = .044$

Note: $L(t)$ is log rosette area, $\hat{L}(t + 1)$ is the fitted value, a is plant age in years, σ_g^2 is the variance about the regression line, and σ_I^2 is the individual-specific heterogeneity in the intercept.

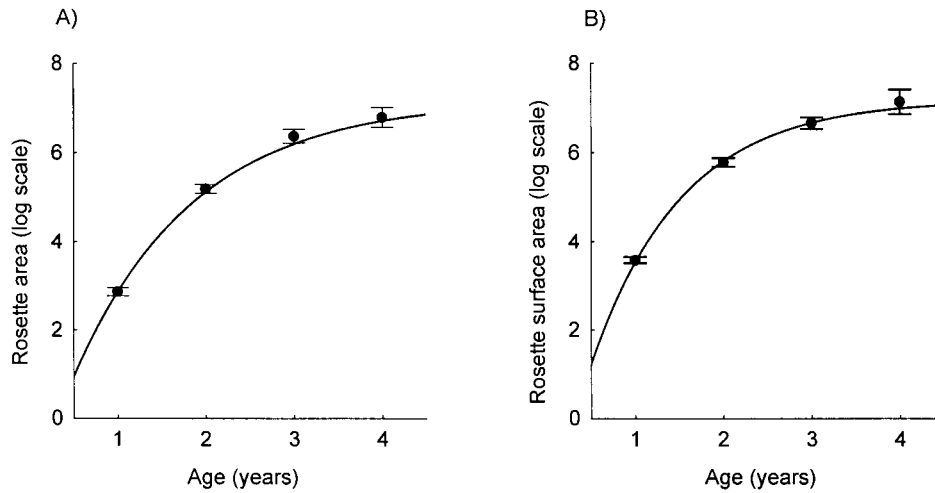


Figure 11: Fitted von Bertalanffy growth curves for (A) the La Crau site and (B) Viols. The vertical bars are a single standard error. Parameter estimates: $L_{\infty} = 7.18$ and $t_0 = 0.31$, while, at La Crau $k = 0.74$ and at Viols $k = 0.98$ ($n = 665$, $r^2 = 0.61$).

use a binomial random variable to determine whether the plant dies, the probability of death being given by the estimated relationship. Those individuals that survive then grow according to the average growth model, with each individual receiving a random growth increment from the estimated distribution of residuals about the fitted line. Individuals smaller than L_s then repeat the cycle of mortality and growth, whereas those that are larger flower. At La Crau, the predicted average size at flowering was $\approx 3,400$ cm^2 , and the predicted average age at flowering was 4.7 yr, while at Viols the predicted average size and age at flowering were $\approx 3,800$ cm^2 and 4.4 yr, respectively. At both sites, the model size predictions are nearly two times the observed values. The observed average ages to flowering were 3.55 and 2.7 yr, at La Crau and Viols, respectively. Again, the model predictions are substantially larger than the observed values.

The 1-yr look ahead is “myopic” in the sense that it ignores all growth opportunities except for those in the following year. For example, in small plants, the expected seed production from waiting 2 yr may be greater than that from waiting 1 yr because of the stochastic variation in growth. So for a given plant size, the optimal decision based on the 1-yr look ahead might be to flower, whereas, with a 2-yr look ahead, the optimal decision might be to wait. We therefore require a technique that allows growth opportunities several years ahead to influence the optimal flowering strategy. Dynamic state variable models, also known as “dynamic programming,” allow this type of calculation to be easily performed (Bellman 1957; Mangel and Clark 1988; Mangel and Ludwig 1992). In appendix

C, we describe a dynamic state variable, DSV, model, which allows the calculation of switch values, L_s , allowing for growth opportunities several years ahead. The predicted switch values are shown in figure 12. Because the plants are short-lived and the variance in growth decreases with plant size, the predicted DSV solutions are well approximated by the 1-yr look-ahead model. The predicted average sizes and ages at flowering, obtained by forward iteration, are $\approx 3,500$ cm^2 and 4.8 yr at La Crau and $\approx 3,800$ cm^2 and 4.4 yr at Viols. Again, model predictions are substantially larger than the observed values.

In these calculations, we have assumed that plants have no information on their u_i values. In contrast, if plants have perfect information on u_i , then we would expect the optimal flowering strategy to vary from plant to plant depending on each individual’s risk of mortality. To explore the effects of this, we calculated the DSV solutions for individuals at La Crau that are ± 2 SDs from the mean of u_i . These plants have average sizes at flowering of $\approx 3,800$ and $\approx 3,200$ cm^2 , whereas plants with no information on u_i flower at $\approx 3,500$ cm^2 . As approximately 95% of individuals lie between these values, it would be difficult to detect these effects from field data. In agreement with this, the estimated individual-specific heterogeneity in intercepts for flowering, σ_p , was not significantly different from 0.

We learn two things from these models: first, scatter about the growth curve selects for larger sizes at flowering and, second, other factors, such as temporal variation in growth and mortality, are likely to be important in determining the optimal flowering strategy. Analytical results

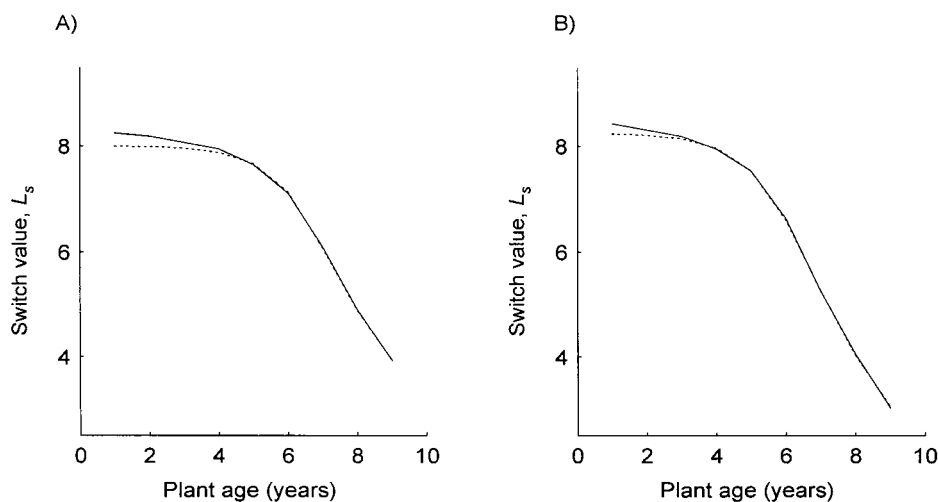


Figure 12: Predicted switch values from the 1-yr look-ahead (*dotted line*) and the dynamic state variable (*solid line*) models at (A) La Crau and (B) Viols.

confirming the first conclusion are presented in Rees et al. (2000).

Individual-Based Models and Genetic Algorithms

In this section, we develop individual-based models that allow the evolution of flowering strategies to be explored in complex models incorporating both individual-specific and temporal variation in demographic parameters. An outline of the model is provided in appendix D. In the model, each plant is characterized by its size, age, and individual-specific growth and mortality parameters. The model includes demographic stochasticity and temporal variation in demographic parameters. Density dependence is incorporated at the recruitment stage by making the number of recruits independent of total seed production. This implies that the probability of an individual seed becoming a recruit is inversely proportional to total seed production.

The simulation model provides an excellent description of the field system, not only in terms of the average population sizes but also the size and age structure of the populations (table 3). The main discrepancy is that the average ages at flowering are larger in the model than in the field. However, in the field data, the age at flowering is consistently underestimated because of the inevitable bias toward plants that flower young: late-flowering plants have a high probability of flowering after the end of the study. In agreement with the data, however, the models predict that plants should flower later at La Crau than at Viols. Because the same data are used to parameterize and to test the models, the agreement between model predic-

tions and the data only demonstrates that the models are a valid description of the system.

We used the simulator to explore the evolution of age- and size-dependent flowering strategies. We did this by introducing a simple genetic algorithm into the model (Sumida et al. 1990). As before, individuals are characterized by size, age, and individual-specific mortality and growth parameters, but each plant also has a flowering strategy. Seeds inherit their parent's flowering strategy plus a small random deviation. In all simulations, we assumed that the offspring strategies were uniformly distributed about the parental strategy. As in the previous models, the number of recruits next year is independent of the seed production this year, but the flowering strategy of each recruit is determined by a fair lottery among seeds. Because the number of recruits each plant produces is determined by a lottery, individual seed production and recruitment are perfectly correlated within a year. In this way, the flowering strategies of the recruits reflect the relative reproductive success of the different flowering strategies in the population.

We explored the evolution of flowering strategies by allowing each of the three aspects of the flowering strategy (the intercept, β_0 , slope of the relationship with size, β_s , and slope of the relationship with age, β_a) to evolve independently, with the other two treated as fixed. Starting with the estimated values and allowing each parameter to evolve, we obtained the results given in table 4. In all cases, the agreement between the theoretical predictions and the estimated parameters was excellent; in addition, the estimated sizes at flowering were extremely close to the data. This agreement may reflect weak selection, and so, by

Table 3: Simulation model predictions and field data from La Crau and Viols

	La Crau		Viols	
	Data	Model	Data	Model
Average number of plants	176	182	240	285
Average size (cm ²)	325 (282, 369)	306 ...	470 (417, 522)	474 ...
Average age (yr)	1.90–2.36	1.9	1.93–2.63	1.8
Average age at flowering (yr)	3.55 (3.0, 4.1)	4.1 ...	2.7 (2.6, 2.9)	3.5 ...
Average size at flowering (cm ²)	1,736 (1,549, 1,922)	1,755 ...	2,208 (2,005, 2,410)	2,235 ...

Note: The figures in parentheses are the 95% confidence intervals.

starting with the estimated parameter values, the models never evolve to strategies of higher fitness simply because this takes a long time. We explored this possibility by using a wide range of starting values and looking for convergence. For the La Crau site, typical model trajectories are shown in figure 13. In each case, we see convergence to the estimated parameter values.

The complex model seems to capture correctly the selective forces acting on the flowering strategy of *Onopordum*. What happens when all three parameters are allowed to evolve? Before looking at the outcome of the model, it is important to understand the statistical properties of the parameters that define the probability of flowering surface. The matrix of correlation coefficients for the parameter estimates is

$$\begin{matrix} & \beta_0 & \beta_s \\ \beta_s & -0.96 & \\ \beta_a & -0.30 & 0.04 \end{matrix},$$

demonstrating that β_0 and β_s are highly negatively correlated. Therefore, as the intercept β_0 increases, the size slope, β_s , can be decreased with little change in the fit of the model. For example, if we fix the intercept at -15 , the estimated value of β_s changes to 1.7, and the percentage of the deviance explained changes by only 3% (from 60% to 57%). This means that we would expect a range of negatively correlated parameter values to give approximately equal fitness because they all describe essentially the same surface. When the fitness of different flowering strategies is approximately equal, evolution is extremely slow.

When all three of the parameters, which define the flowering surface, were allowed to evolve, the predicted average sizes at reproduction were 1,924 and 2,394 cm² at La Crau and Viols, respectively, slightly larger than observed in the field. However, the predicted parameter values are considerably larger than those estimated from the field (see table 5). Despite the large differences between the pre-

dicted parameters and the estimated ones, the flowering strategies were similar (see fig. 14). The predicted relationship at both sites approaches a step function, which results in the expected average size at flowering being larger than measured in the field.

Sensitivity Analysis

To explore how the model predictions were influenced by the different types of variability, we performed a sensitivity analysis. This is divided into two sections: the first deals with temporal variation in model parameters, the second with other forms of variability.

Temporal Variation. Four different environmental scenarios were used to explore the effects of temporal variation in growth and mortality. Specifically, we evaluated the effects of temporal variation in growth and mortality by comparing the predictions obtained using the average and yearly models in the simulation; the results are given in table 5. Clearly, temporal variation in mortality has little

Table 4: Predicted and estimated parameters for the flowering strategy at each of the two sites

Site	Parameter			Average size at flowering (cm ²)
	β_0	β_s	β_a	
La Crau	-24.05	1,818
Viols	-23.73	2,200
La Crau	...	2.84	...	1,765
Viols	...	2.90	...	2,170
La Crau85	1,749
Viols92	2,193
Estimated value	-23.73	2.87	.85	...

Note: Each parameter is allowed to evolve assuming the others are fixed. The final column gives the average size at flowering predicted by the model.

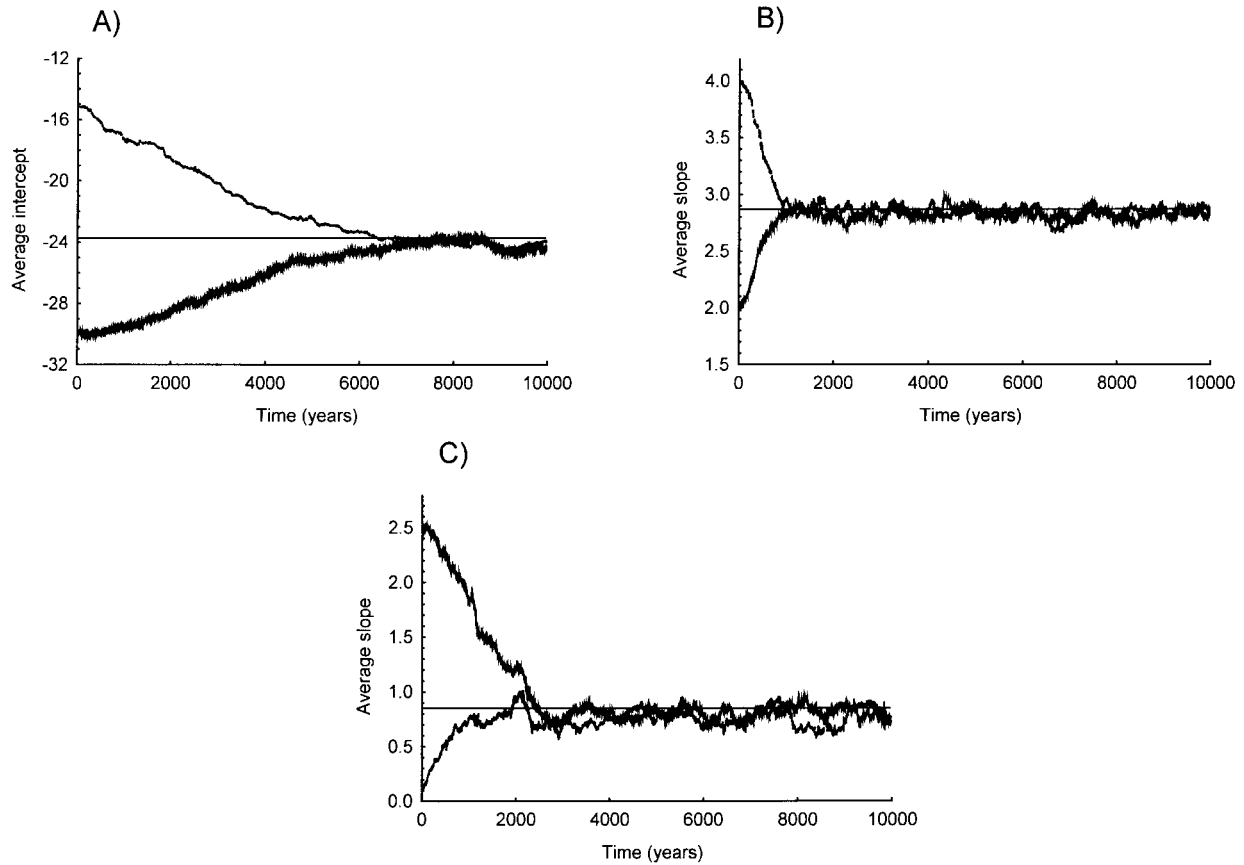


Figure 13: Evolutionary trajectories for (A) the intercept, β_0 ; (B) the slope of the size relationship, β_s ; and (C) the slope of the age relationship, β_a . In each case, the horizontal line is the estimated parameter value. Other parameter values are for the La Crau site.

effect on the predicted average size and age at flowering. In contrast, temporal variation in growth selects for reduced size and age at flowering. The predicted sizes at flowering in these models are slightly larger than those observed in the field.

The assumption of constant yearly recruitment had little effect on the expected average sizes at flowering. In models with yearly variation in growth and mortality, but constant recruitment, the predicted sizes at flowering were 1,968 and 2,343 cm² at the La Crau and Viols sites, respectively. Both values were extremely close to those obtained with yearly variation in recruitment.

Why is temporal variation in growth so important? The answer to this question is shown in figure 15, which illustrates the expected growth curves of plants of different ages in the yearly growth model and the average growth model. The expected growth curves are calculated by conditioning on plant size in the previous year:

$$\begin{aligned}
 E[L(t+1)|L(t)] &= E[a_g + b_g L(t) + b_a a \\
 &\quad + b_{g2} L(t)^2 + b_{ga} L(t) a + \varepsilon] \\
 &= \bar{a}_g + \bar{b}_g \bar{L}(t) + b_a a \\
 &\quad + b_{g2} \bar{L}(t)^2 + b_{ga} \bar{L}(t) a,
 \end{aligned}
 \tag{14}$$

where a_g , b_g , b_a , b_{g2} , and b_{ga} are estimated regression parameters, and the terms with overbars are averaged quantities. In calculating this expectation, we have used the facts that $E[\varepsilon] = 0$ and $E[XY] = E[X]E[Y]$, providing X and Y are independent. From the figure, it is clear that the expected sizes of plants the following year becomes smaller as plants grow older. Therefore, the expected payoff from delaying reproduction decreases as plants get older, and this selects for smaller sizes at flowering. In contrast, the average model predicts larger asymptotic sizes than the yearly model, and the expected reduction in plant size for

larger plants that do not flower is smaller. Does the average of the yearly growth model, equation (14), correctly capture the selective forces operating, or are the fluctuations in a_g and b_g important? We explored this by using equation (14) in the simulation model. The predicted average sizes at flowering, using the yearly mortality model and with recruitment varying from year to year, were 2,300 and 2,600 cm² at La Crau and Viols, respectively. The changes in the average sizes at flowering assuming different forms of temporal variation in growth may be summarized as follows:

$$\text{La Crau } 1,924 (R) \rightarrow 2,300 (\bar{R}) \rightarrow 2,764 (C)$$

$$\text{Viols } 2,394 (R) \rightarrow 2,600 (\bar{R}) \rightarrow 3,625 (C),$$

where (R) is the predicted average size at flowering in an environment with yearly variation in growth, (\bar{R}) the value using equation (14) for growth, and (C) the value assuming no yearly variation in growth. In all cases, we used the yearly mortality model and allowed variation in the number of recruits from year to year. At La Crau, 45% of the effect of temporal variation in growth is a result of age dependence and curvature of the growth surface (i.e., eq. [14]). In contrast, at Viols, 83% of the effect of temporal variation in growth parameters is a direct result of parameter fluctuation from year to year, and only 13% can be attributed to age-dependent and curvature effects.

Other Forms of Variability. Assuming no variation about the growth curve ($\sigma_g^2 = 0$) resulted in expected sizes at flowering of 1,050 and 1,500 cm² at the La Crau and Viols sites, respectively. Clearly, variation about the growth curve selects for larger sizes at flowering, as found in the 1-yr look-ahead and dynamic state variable models. How does individual-specific heterogeneity in growth and mortality affect the flowering strategy? For growth, this is easily as-

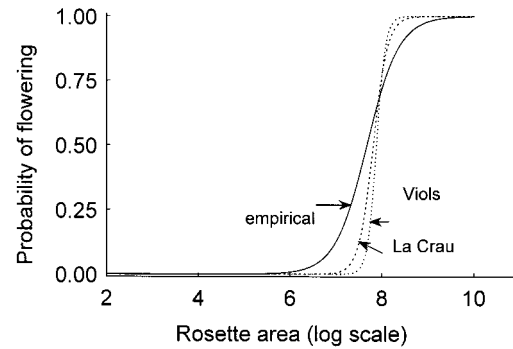


Figure 14: Empirical and predicted flowering strategies for 2-yr-old plants at La Crau and Viols. The predicted flowering strategies are from a model with temporal variation in growth, mortality, and recruitment. See text for details and table 5 for parameter values.

essed by setting the individual-specific heterogeneity in the intercepts to 0 ($\sigma_i^2 = 0$). In models with yearly variation in growth, mortality, and recruitment but no individual-specific heterogeneity in the intercepts of the growth equation, the predicted sizes at flowering, were 2,036 and 2,409 cm² at the La Crau and Viols sites, respectively. Both values were extremely close to those obtained assuming individual-specific heterogeneity in the growth equation intercepts (table 5).

To explore the effects of individual-specific heterogeneity in the intercepts of the mortality model is more complicated because the average mortality function, for a given size and age, does not equal the mortality function of an individual with the average intercept (i.e., $u_i = 0$; see fig. 5). To overcome this problem we evaluated the integral in equation (1) over a wide range of ages and sizes and fitted a logistic function to the resulting probability surface. This surface defines the average mortality function for a given age and size. We then set σ_a equal to 0 and used the average mortality function in the simulation. The

Table 5: Effects of temporal variation in growth and mortality on the predicted flowering strategy, and average size and age at flowering

Site	Growth	Mortality	β_0	β_s	β_a	Average size at flowering	Average age at flowering
La Crau	C	C	-60.8	6.5	2.7	2,716	4.6
Viols	C	C	-62.4	6.6	2.9	3,312	3.5
La Crau	C	R	-52.7	5.9	1.7	2,764	4.7
Viols	C	R	-66.7	7.6	1.7	3,625	4.4
La Crau	R	C	-48.7	6.0	1.4	1,978	3.9
Viols	R	C	-48.1	5.9	1.9	2,345	3.1
La Crau	R	R	-54.8	6.4	2.4	1,924	4.1
Viols	R	R	-92.2	10.3	5.5	2,394	3.5

Note: C = average model with no yearly variation, R = yearly model with temporal variation.

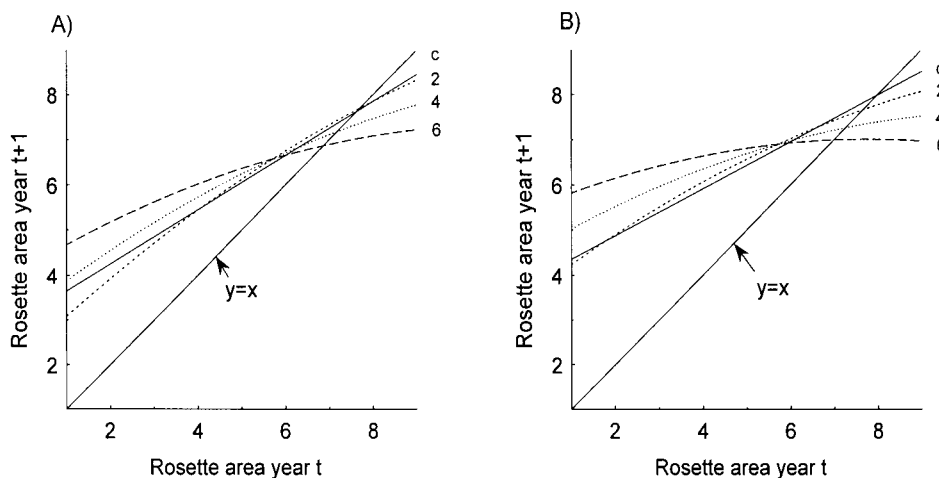


Figure 15: Average growth curves for the average and yearly models at (A) La Crau and (B) Viols; c = average model, and numerals indicate plant age. For reference, the one-to-one line, $y = x$, is shown. The asymptotic size, at a given age, occurs where this line crosses the growth line.

predicted average sizes at flowering were 1,890 and 2,253 cm^2 at La Crau and Viols, respectively. Both values are very similar to those obtained in models incorporating individual-specific heterogeneity in the intercepts of the mortality model (see table 5). Clearly the model predictions are insensitive to the estimated levels of individual-specific variability.

Discussion

The individual-based simulation models for *Onopordum* illustrate that complex age- and size-structured models can be constructed using easily obtained field data. These models provide a surprisingly good description of average population size and population size and age structure. For parameter estimation, it is important to quantify the systematic changes in demographic parameters with size and age and the variance about the estimated curve. The variance about the growth curve, σ_g^2 , has a dramatic effect on the size structure of the population, particularly the size structure of those plants that flower. The reason for this is straightforward: those plants that have large positive residuals become very large and so will be almost certain to flower. In contrast, those plants that have large negative residuals become small and are very unlikely to flower. There is therefore a fundamental asymmetry in the way this variance term influences the size of plants that flower. Temporal variation in the growth parameters is also important and, in contrast to σ_g^2 , selects for smaller sizes at flowering because delaying reproduction becomes more risky.

Ignoring the variance about the growth curve leads to

inaccuracies in the ecological models, and this has inevitable effects on the evolutionary predictions from these models. The simple analytical models, based on maximizing R_0 , give answers close to those obtained from the genetic algorithm and DSV models when there is no variance about the growth line. A more detailed description of the relationships between the models is given in Rees et al. (2000). However, when there is substantial variance about the growth curve, the approaches diverge considerably. The presence of substantial variance about the growth curve means that size and age are no longer tightly coupled. This, combined with the fact that in most plants fecundity is determined by size not age, means that size is a better cue for reproduction than age. In agreement with this expectation, flowering in many monocarpic species is strongly related to size but only weakly related to age (Werner 1975; Baskin and Baskin 1979; van der Meijden and van de Waals-Kooi 1979; Gross 1981; Hirose and Kachi 1982; Klemow and Raynal 1985; de Jong et al. 1986; Lacey 1986a, 1986b; Bullock et al. 1994; Klinkhamer et al. 1996; Wesselingh and Klinkhamer 1996). However, strict biennials do occur, and these species seem to have age-dependent flowering (Kelly 1985a). In the strict biennial *Gentianella amarella*, all surviving plants flowered in their second year, with the result that many plants flowered while very small and so failed to set seed (Kelly 1989a, 1989b). In other species with age-dependent flowering, such as bamboos, delays in reproduction have been linked with mast seeding and predator satiation (Janzen 1976).

However, several variance terms had little impact on the model predictions: these were temporal variation in the number of recruits, temporal variation in mortality pa-

rameters, and individual-specific heterogeneity in growth and mortality intercepts (σ_i^2 and σ_d^2). Temporal variation in mortality has a similar effect to variation in the number of recruits from year to year because mortality acts primarily on small, new recruits (see fig. 4). Both types of variability can generate a bet-hedging component to fitness, although the effects found here, and in other studies (de Jong et al. 1989), were small. This is because in species with size-dependent flowering strategies where there is substantial variance about the growth curve, σ_g^2 , the timing of flowering within a cohort is spread over several years. For example, in *Onopordum* individuals flowered at all ages between 2 and 5 yr.

The estimated individual-specific heterogeneity in the intercepts of the growth curve, σ_i^2 , was extremely small, and so it is perhaps not surprising that it had little effect on the model predictions. However, there was substantial individual-specific heterogeneity about the mortality curve, σ_b , and this had little effect on the model predictions. To see why this is, note that most plants flower at about 2,000 cm² (fig. 2), which on a log scale corresponds to ≈ 7.5 . At large sizes two factors become important: first, the individual-specific heterogeneity in the intercepts of the mortality curve translates into small changes in the probability of death and, second, the logistic mortality curve is approximately linear (see fig. 5). With approximate linearity and small changes in the probability of death between individuals, the effects of individual-specific heterogeneity in the intercepts of the mortality curve are small.

Several features of the biology were not included in the models, most notably genetic structure and consideration of fitness through male function. In *Cynoglossum officinale*, small plants allocate relatively more to male function (pollen) than large plants (Klinkhamer and de Jong 1993). This could have important implications for the flowering strategy, as the fitness of small plants could be greater than predicted from a consideration of seed set alone. This would lead to smaller predicted sizes at flowering. However, given the accuracy of the model predictions, the effect of ignoring male function appears to be minimal.

The genetic basis of size-dependent regulation of flowering has been explored in two species: *Senecio jacobaea* and *C. officinale* (Wesselingh and de Jong 1995; Wesselingh and Klinkhamer 1996). In both species artificial selection experiments demonstrate that substantial genetic variance exists in natural population for the threshold size for flowering. For example, in *Cynoglossum*, the parental generation had highly variable threshold sizes for flowering (2.6–13.4 g). After a single generation of selection for low threshold sizes, all plants flowered at <3.2 g, whereas in the high selection line no plants flowered <3.6 g. In studies of the geographical variation in threshold sizes for flow-

ering, extremely steep relationships between the probability of flowering and plant size have been found in *Cynoglossum* populations, particularly those from botanical gardens (Wesselingh et al. 1993). This could be the result of truncation selection: all plants that fail to flower in their second year die because of cultivation or genetic drift caused by small population sizes (Wesselingh et al. 1993). These results suggest that in *Cynoglossum* genetic constraints do not prevent the plant from achieving a step function relationship between the probability of flowering and plant size.

The most accurate predictions come from models where the shape of the flowering surface is constrained along two of the three axes (table 4). Allowing all parameters to evolve results in a step function relationship between the probability of flowering and plant size (fig. 14). There are several possible reasons why the observed relationship might be shallower than that predicted by the models. The simplest explanation is that flowering decisions are made several months before plants actually flower (Werner 1975; Baskin and Baskin 1979; de Jong et al. 1986; Klinkhamer et al. 1987). If growth in the interval between the decision and flowering varies between individuals, then a range of sizes at flowering would be observed. This between-plant variation in size at flowering would occur even if all plants had exactly the same switch value for flowering. The second possible explanation is that plants respond to spatial variation in mortality or growing conditions, and the spread of flowering sizes then represents an adaptive response to this spatial variation. This explanation seems unlikely, as there was no significant individual-specific heterogeneity in intercepts for flowering ($\sigma_f = 0$). A third possible explanation is that flowering strategies vary from year to year and that, by pooling across years, we generate variability in the flowering relationship. This explanation also seems unlikely given that year effects only accounted for 2% of the deviance in the probability of flowering. It is possible that genetic constraints result in a graded relationship between plant size and the probability of flowering. We have no information on the genetic basis of flowering in *Onopordum*, but other studies, discussed above, suggest that plants can achieve step function relationships between the probability of flowering and plant size. The final explanation is that, when all three parameters are allowed to evolve, the rate of evolution becomes very slow and that the flowering patterns we see in the field represent a snapshot of an ongoing evolutionary process.

Given the importance of temporal variation in growth parameters, how can accurate predictions be made from such a short run of census data? It is possible, but unlikely, that the temporal variation observed is representative of the long-term environment in which the plants evolved.

A more likely explanation is that the flowering decisions depend on the growing conditions in a particular year. In agreement with this, there was a significant, although small, year effect on the probability of flowering. With longer runs of data, it should be possible to look for yearly variation in the flowering strategy and relate this to the growing conditions. Using a 20-yr data set on *Carlina vulgaris*, we are currently exploring this possibility.

The von Bertalanffy model produces simple analytical results, which correctly predict the direction of selection in the more complex models. However, the predictions of the von Bertalanffy model need to be interpreted with care. For example, when moving from unproductive to productive habitats, we would expect both L_∞ and k to increase, and so the ESS flowering size, given by equation (10), should increase. In *Onopordum* (fig. 2) and *Carlina vulgaris* (Klinkhamer et al. 1996), the average size at flowering is indeed larger in habitats that are more productive.

However, in these species the flowering strategy (relationship between the probability of flowering and plant size; see fig. 6) does not vary between productive and unproductive habitats. Differences in size at flowering are the result of variation in growth rates and not changes in flowering strategy as predicted by the model. Clearly, great care is needed when testing general theoretical models and alternative models must be explored (Charlesworth 1994).

Acknowledgments

We should like to thank T. de Jong, N. Kachi, D. Kelly, J. Kozłowski, and L. Turnbull for comments on the manuscript. We should particularly like to thank A. Sih, who summarized the referees' views and provided detailed, specific comments that considerably improved the manuscript.

APPENDIX A

Table A1: Main parameters and variables used in the statistical and mathematical models

Symbol	Meaning
$L(t)$	Log rosette area in year t
m_0	Intercept of logistic mortality equation
m_s	Size-dependent slope of logistic mortality equation
m_a	Age-dependent slope of logistic mortality equation
u_i	Individual-specific heterogeneity term in logistic mortality equation
σ_u^2	Variance of u_i , individual-specific heterogeneity in mortality
$g(u_i)$	Probability density function of u_i (Gaussian)
β_0	Intercept of logistic flowering equation
β_s	Size-dependent slope of logistic flowering equation
β_a	Age-dependent slope of logistic flowering equation
σ_f^2	Variance in individual-specific heterogeneity in flowering
a_g	Intercept of growth model
b_g	Size-dependent slope of growth model
b_0	Slope term of growth model, the subscripts indicating age- or size-dependence
ε	Residual about growth curve
$f(\varepsilon)$	Probability density function of ε (Gaussian)
σ_ε^2	Variance of residuals about growth curve
σ_I^2	Variance representing individual specific heterogeneity in growth
L_∞	Asymptotic size in von Bertalanffy equation
k	Rate parameter in von Bertalanffy equation
t_0	Hypothetical age at which size would be 0 in von Bertalanffy equation
p, m	Parameters of exponential mortality model
A, B	Intercept and slope of fecundity equation
\tilde{t}, \tilde{L}	ESS age and size at flowering from von Bertalanffy equation
L_s	Switch-value for flowering

APPENDIX B

Logistic-Normal Statistical Models

Here we briefly describe the logistic-normal models used in the analysis of the probability of flowering and mortality. Assume we have m plants each observed on n_i occasions, the subscript denoting the i th plant. Then, for a standard logistic regression, the probability of flowering is

$$p_{ij}(\beta_0, \beta_1, x_{ij}) = \frac{\exp(\beta_0 + \beta_1 x_{ij})}{1 + \exp(\beta_0 + \beta_1 x_{ij})}, \quad (\text{B1})$$

where the β 's are estimated parameters and x_{ij} is an explanatory variable for the i th plant at the j th time. Here, for simplicity, we have assumed that there is only one explanatory variable but that the ideas extend naturally to multiple explanatory variables and interactions. For the standard logistic regression, the likelihood of the data is then

$$L(\beta; \mathbf{y}) = \prod_i^m \prod_j^{n_i} p_{ij}(\beta_0, \beta_1, x_{ij})^{y_{ij}} [1 - p_{ij}(\beta_0, \beta_1, x_{ij})]^{1-y_{ij}}, \quad (\text{B2})$$

where \mathbf{y} is the vector of observed values of y_{ij} (see Cox and Snell 1989). Now we assume there are random effects that influence each plant. If we had long runs of data on each plant, these could be estimated and their variation studied. However, we only have a small number of observations on each plant and so must use information across plants to make inferences about individual-specific heterogeneity. Specifically, we will assume that each plant has its own regression intercept of the form $\beta_0 + u_i$ and that the u_i values are drawn from a distribution that describes individual-specific heterogeneity. We can then write

$$p_{ij}(\beta_0, \beta_1, u_i, x_{ij}) = \frac{\exp(\beta_0 + u_i + \beta_1 x_{ij})}{1 + \exp(\beta_0 + u_i + \beta_1 x_{ij})}, \quad (\text{B3})$$

which is the individual-specific probability of flowering. To complete the model specification, we need to assume a parametric model for u_i ; specifically, we assume that u_i follows a Gaussian distribution with 0 mean and standard deviation σ . The likelihood then becomes

$$L(\beta_0, \beta_1, \sigma; \mathbf{y}) = \prod_i^m \int f(u_i) \prod_j^{n_i} p_{ij}(\beta_0, \beta_1, u_i, x_{ij})^{y_{ij}} [1 - p_{ij}(\beta_0, \beta_1, u_i, x_{ij})]^{1-y_{ij}} du_i, \quad (\text{B4})$$

where $f(u_i)$ is the Gaussian probability density function. Numerical methods can then be used to maximize this and so obtain parameter estimates. In this way, we may obtain useful information on individual-specific heterogeneity in the probability of flowering. This is quantified by the estimated standard deviation of the distribution of u_i . The computer package SABRE provides routines for fitting this type of model (Stott et al. 1996). The effects of misspecifying the mixture distribution (i.e., $f(u_i)$) are discussed in Neuhaus et al. (1992). These authors show that, when the mixture distribution is misspecified, estimates of model parameters, including the effects of covariates, are typically asymptotically biased, that is, inconsistent. However, the magnitude of the bias is generally small, and so valid estimates of covariate effects can be obtained when the mixture distribution is misspecified. This is important as there are often problems identifying the exact form of the mixing distribution (Hougaard 1984).

APPENDIX C

Dynamic State Variable Models

We now briefly describe a dynamic state variable model (DSV; Mangel and Clark 1988; Mangel and Ludwig 1992) to determine the switching value. To do this, let

$$F(L, t) = \text{the expected fitness of a plant of log area, } L, \text{ at age } t. \quad (\text{C1})$$

We assume there is a time T at which the plant must reproduce, so that

$$F(L, T) = \exp(A + BL). \quad (\text{C2})$$

The terminal time T can be interpreted alternatively as the time of reproductive senescence or the time at which successional changes make reproduction mandatory. Most of our results will deal with tT , in which case the switching values are independent of T (i.e., stationary, *sensu* Mangel and Clark 1988).

For times before T , $F(L, t)$ is determined by comparison of current reproduction with the expected value of future reproduction, taking growth and survival into account. The fitness value (measured in terms of expected reproduction) $V_{\text{now}}(L, t)$ of reproducing at age t for a plant of size L is

$$\begin{aligned} V_{\text{now}}(L, t) &= \text{seed production of a plant of size } L \\ &= \exp(A + BL). \end{aligned} \quad (\text{C3})$$

The fitness value of continuing to grow is

$$\begin{aligned} V_{\text{grow}}(L, t) &= \text{average fitness of a plant that grows and survives} \\ &= \int \int f(\varepsilon)g(u_i)s(a_g + b_gL + \varepsilon, u_i)F(a_g + b_gL + \varepsilon, t + 1)du_id\varepsilon, \end{aligned} \quad (\text{C4})$$

where $s(a_g + b_gL + \varepsilon, u_i)$ is the logistic survival function. Note that this differs from equation (12) in that we calculate the expectation of $F(L, t + 1)$, which depends on the relative fitness gains from immediate reproduction or reproduction at some time in the future. In light of the definition of $F(L, t)$, we have the dynamic iteration equation

$$F(L, t) = \max\{V_{\text{now}}(L, t), V_{\text{grow}}(L, t)\}. \quad (\text{C5})$$

This equation is solved backward in time, and the switching value L_s is the value at which $V_{\text{now}}(L_s, t) = V_{\text{grow}}(L_s, t)$. Note that if $t = T - 1$, then the switching value predicted by using equations (C3), (C4), and (C5) must equal the value obtained using the 1-yr look ahead (eq. [12]). The approaches are equal in this case because there is only one opportunity for growth at time $T - 1$.

APPENDIX D

Individual-Based Simulation Models

Here we briefly outline the construction of the individual-based simulation model. In the simulator, each plant is characterized by its size, age, and individual-specific growth and mortality parameters. Plants behave according to the statistical rules described in the main body of the article. Note that size in the model is a continuous variable; we do not divide the population into categories. Events in the simulation model occur in the following order: First, year type is selected, which determines the number of recruits and the yearly parameters for the growth and mortality functions. Second, individuals die with a probability depending on their size, age, and individual-specific intercept. Third, plants that did not die then flower with a probability depending on their size and age. Fourth, those plants that neither died

nor flowered grow according to the growth equation. Finally, recruits are added to the system. Each of these steps is stochastic, so, if a particular plant has a 0.3 probability of death, then a uniform random number is generated and, if this is <0.3 , the plant is killed; otherwise it survives. In a similar way, we determine whether or not a plant reproduces. When applying the growth equation, we included the residual variation from the regression equation by adding random normal deviates with 0 mean and standard deviation set by the data. Individual-specific effects were incorporated by assigning each recruit a standard normal deviate with standard deviation set by the data. In this way, two plants of the same size could grow by different amounts just as in the real data. We did not include any effects of the local competitive environment on mortality or growth for two reasons: first, this would require a much more complicated model with explicit space, and in order to construct this we would need information on seed dispersal and the distribution of germination microsites, and second, these forms of density dependence only slightly increased the explanatory power of the regression models, whereas the uncoupling of recruitment from seed production is a very strong form of density dependence.

The number of recruits added to the system was drawn from the observed distribution of recruits, at each site, over the period 1989–1991. Consecutive values were selected independently, and all observed values are assumed equally likely. In this way, the number of recruits varied from year to year and was independent of seed production. The initial sizes of the recruits were determined by the distribution of sizes observed in each of the populations.

In all simulations, we used the random number routines given in Press et al. (1990). Most numerical results presented are averages of the last 2,000 years of a 10,000-yr simulation. However, when all three parameters that define the flowering surface were allowed to evolve, the simulations converged much slower, and so the results presented are averages of the last 2,000 years of a 200,000-yr simulation.

Literature Cited

- Allan, C. J., and P. J. Holst. 1996. Longevity of soil based seeds of *Onopordum illyricum*. *Plant Protection Quarterly* 11:242.
- Baskin, J. M., and C. M. Baskin. 1979. Studies on the autecology and population biology of the weedy monocarpic perennial, *Pastinaca sativa*. *Journal of Ecology* 67:601–610.
- Becker, R. A., J. M. Chambers, and A. R. Wilks. 1988. *The new S-Language*. Chapman & Hall, New York.
- Bell, G. 1980. The costs of reproduction and their consequences. *American Naturalist* 116:45–76.
- Bellman R. 1957. *Dynamic programming*. Princeton University Press, Princeton, N.J.
- Briese, D. T., D. Lane, B. H. Hyde-Wyatt, J. Crocker, and R. G. Diver. 1990. Distribution of thistles of the genus *Onopordum* in Australia. *Plant Protection Quarterly* 5: 23–27.
- Briese, D. T., A. W. Sheppard, H. Zwölfer, and P. E. Boldt. 1994. Structure of the phytophagous insect fauna of *Onopordum* thistles in the northern Mediterranean basin. *Biological Journal of the Linnean Society* 53: 231–253.
- Bullock, J. M., B. C. Hill, and J. Silvertown. 1994. Demography of *Cirsium vulgare* in a grazing experiment. *Journal of Ecology* 82:101–111.
- Bulmer, M. G. 1985. Selection for iteroparity in a variable environment. *American Naturalist* 126:63–71.
- Caswell, H., and P. A. Werner. 1978. Transient behaviour and life history analysis of teasel (*Dipsacus sylvestris* Huds). *Ecology* 59:53–66.
- Cavers, P. B., R. H. Groves, and P. E. Kaye. 1995. Seed population dynamics of *Onopordum* over one year in southern New South Wales. *Journal of Applied Ecology* 32:425–433.
- Charlesworth, B. 1994. *Evolution in age-structured populations*. Cambridge University Press, Cambridge.
- Charnov, E. L. 1993. *Life-history invariants: some explorations of symmetry in evolutionary biology*. Oxford University Press, Oxford.
- Charnov, E. L., and W. M. Schaffer. 1973. Life history consequences of natural selection: Cole's result revisited. *American Naturalist* 107:791–793.
- Cole, L. C. 1954. The population consequences of life history phenomena. *Quarterly Review of Biology* 29: 103–137.
- Cox, D. R., and E. J. Snell. 1989. *Analysis of binary data*. Chapman & Hall, London.
- Crouch, A. C., and E. Spiegelman. 1990. The evaluation of integrals of the form: application to logistic-normal models. *Journal of the American Statistical Association* 85:464–469.
- de Jong, T. J., and P. G. L. Klinkhamer. 1986. Population ecology of the biennials *Cirsium vulgare* and *Cynoglossum officinale*: an experimental and theoretical approach. Ph.D. thesis. University of Leiden.
- de Jong, T. J., P. G. L. Klinkhamer, and A. H. Prins. 1986. Flowering behavior of the monocarpic perennial *Cynoglossum officinale* L. *New Phytologist* 103:219–229.
- de Jong, T. J., P. G. L. Klinkhamer, and J. A. J. Metz. 1987. Selection for biennial life histories in plants. *Vegetatio* 70:149–156.
- de Jong, T. J., P. G. L. Klinkhamer, S. A. H. Geritz, and

- E. van der Meijden. 1989. Why biennials delay flowering: an optimization model and field data on *Cirsium vulgare* and *Cynoglossum officinale*. *Acta Botanica Neerlandica* 38:41–55.
- Diggle, P. J., K. Y. Liang, and S. L. Zeger. 1996. Analysis of longitudinal data. Oxford Scientific, Oxford.
- Goss, W. L. 1924. The vitality of buried seeds. *Journal of Agricultural Research* 29:349–362.
- Gross, K. L. 1981. Predictions of fate from rosette size in four “biennial” plant species: *Verbascum thapsus*, *Oenothera biennis*, *Daucus carota*, and *Tragopogon dubius*. *Oecologia* (Berlin) 48:209–213.
- Gross, R. S., and P. A. Werner. 1983. Probabilities of survival and reproduction relative to rosette size in the common burdock (*Arctium minus*, Compositae). *American Midland Naturalist* 109:184–193.
- Groves, R. H., J. J. Burdon and K. P. E. 1990. Demography and genetics of *Onopordum* in southern New South Wales. *Journal of Ecology* 78:47–55.
- Hastings, A. 1978. Evolutionary stable strategies and the evolution of life histories. I. Density dependent models. *Journal of Theoretical Biology* 75:527–536.
- Hirose, T., and N. Kachi. 1982. Critical plant size for flowering in biennials with special reference to their distribution in a sand dune system. *Oecologia* (Berlin) 55: 281–284.
- . 1986. Graphical analysis of the life-history evolution of *Oenothera glazioviana* Micheli. *Oecologia* (Berlin) 68:490–495.
- Hougaard, P. 1984. Life table methods for heterogeneous populations: distributions describing the heterogeneity. *Biometrika* 71:75–83.
- Janzen, D. H. 1976. Why bamboos wait so long to flower. *Annual Review of Ecology and Systematics* 7:347–391.
- Kachi, N. 1990. Evolution of size-dependent reproduction in biennial plants: a demographic approach. Academic Press, London.
- Kachi, N., and T. Hirose. 1985. Population-dynamics of *Oenothera glazioviana* in a sand-dune system with special reference to the adaptive significance of size-dependent reproduction. *Journal of Ecology* 73:887–901.
- Kawecki, T. J. 1993. Age and size at maturity in a patchy environment: fitness maximization versus evolutionary stability. *Oikos* 66:309–317.
- Kelly, D. 1985a. On strict and facultative biennials. *Oecologia* (Berlin) 67:292–294.
- . 1985b. Why are biennials so maligned? *American Naturalist* 125:473–497.
- . 1989a. Demography of short-lived plants in chalk grassland. I. Life-cycle variation in annuals and strict biennials. *Journal of Ecology* 77:747–769.
- . 1989b. Demography of short-lived plants in chalk grassland. II. Control of mortality and fecundity. *Journal of Ecology* 77:770–784.
- Klemow, K. M., and D. J. Raynal. 1985. Demography of two facultative biennial plant species in an unproductive habitat. *Journal of Ecology* 73:147–167.
- Klinkhamer, P. G. L., and T. J. de Jong. 1983. Is it profitable for biennials to live longer than two years? *Ecological Modelling* 20:223–232.
- . 1987. Plant size and seed production in the monocarpic perennial *Cynoglossum officinale*. 1. *New Phytologist* 106:773–783.
- . 1993. Phenotypic gender in plants: effects of plant size and environment on allocation to seeds and flowers in *Cynoglossum officinale*. *Oikos* 67:81–86.
- Klinkhamer, P. G. L., T. J. de Jong, and E. Meelis. 1987. Delay of flowering in the biennial *Cirsium vulgare*: size effects and devernialization. *Oikos* 49:303–308.
- Klinkhamer, P. G. L., T. J. de Jong, and J. L. H. de Heiden. 1996. An eight-year study of population-dynamics and life-history variation of the biennial *Carlina vulgaris*. *Oikos* 75:259–268.
- Kozłowski, J., and M. Janczur. 1994. Density-dependent regulation of population number and life-history evolution: optimization of age at maturity in a simple allocation model for annuals and biennials. *Ecological Modelling* 73:81–96.
- Lacey, E. P. 1986a. The genetic and environmental-control of reproductive timing in a short-lived monocarpic species *Daucus carota* (Umbelliferae). *Journal of Ecology* 74:73–86.
- . 1986b. Onset of reproduction in plants: size versus age-dependency. *Trends in Ecology & Evolution* 1: 72–75.
- . 1988. Latitudinal variation in reproductive timing of a short-lived monocarp, *Daucus carota* (Apiaceae). *Ecology* 69:220–232.
- Lacey, E. P., L. Real, J. Antonovics, and D. G. Heckel. 1983. Variance models in the study of life histories. *American Naturalist* 122:114–131.
- Mangel, M. 1996. Life-history invariants, age at maturity and the ferox trout. *Evolutionary Ecology* 10:249–263.
- Mangel, M., and C. W. Clark. 1988. Dynamic modeling in behavioral ecology. Princeton University Press, Princeton, N.J.
- Mangel, M., and D. Ludwig. 1992. Definition and evaluation of the fitness of behavioral and developmental programs. *Annual Review of Ecology and Systematics* 23:507–536.
- Mylius, S. D., and O. Diekmann. 1995. On evolutionarily stable life-histories, optimization and the need to be specific about density-dependence. *Oikos* 74:218–224.
- Neuhaus, J. M., J. D. Kalbfleisch, and W. W. Hauck. 1991. A comparison of cluster-specific and population-aver-

- aged approaches for analyzing correlated binary data. *International Statistical Review* 59:25–35.
- Neuhauser, J. M., W. W. Hauck, and J. D. Kalbfleisch. 1992. The effects of mixture distribution mis-specification when fitting mixed-effects logistic-models. *Biometrika* 79:755–762.
- Pacala, S. W., and J. A. Silander. 1987. Neighborhood interference among velvet leaf, *Abutilon theophrasti*, and pigweed, *Amaranthus retroflexus*. *Oikos* 48:217–224.
- Pettit, W. J., D. T. Briese, and A. Walker. 1996. Aspects of thistle population dynamics with reference to *Onopordum*. *Plant Protection Quarterly* 11:232–235.
- Press, W. H., B. P. Flannery, S. A. Teukolsky, and W. T. Vetterling. 1990. *Numerical recipes in Pascal: the art of scientific computing*. Cambridge University Press, Cambridge.
- Rees, M., and M. J. Crawley. 1989. Growth, reproduction and population-dynamics. *Functional Ecology* 3: 645–653.
- Rees, M., and M. J. Long. 1993. The analysis and interpretation of seedling recruitment curves. *American Naturalist* 141:233–262.
- Rees, M., M. Mangel, L. A. Turnbull, A. Sheppard, and D. Briese. 2000. The effects of heterogeneity on dispersal and colonisation in plants: ecological consequences of habitat heterogeneity. In M. J. Hutchings, E. A. John, and A. J. A. Stewart, eds. *Ecological consequences of environmental heterogeneity*. Blackwell, Oxford.
- Reinartz, J. A. 1984. Life-history variation of common mullein (*Verbascum thapsus*). 1. Latitudinal differences in population-dynamics and timing. *Journal of Ecology* 72:897–912.
- Roff, D. A. 1984. The evolution of life-history parameters in teleosts. *Canadian Journal of Fisheries and Aquatic Sciences* 41:989–1000.
- . 1986. Predicting body size with life-history models. *BioScience* 36:316–323.
- . 1992. *The evolution of life histories: theory and analysis*. Chapman & Hall, London.
- Ross, G. J. S. 1990. *Nonlinear estimation*. Springer, London.
- Sheppard, A. W. 1996. The Cardueae: weeds and the impact of natural enemies for biological control. *Proceedings of the International Compositae Conference*, Kew, 1994. Royal Botanic Gardens, Kew.
- Stearns, S. C. 1992. *The evolution of life histories*. Oxford University Press, Oxford.
- Stefanski, L. A., and R. J. Carroll. 1985. Covariate measurement error in logistic regression. *Annals of Statistics* 13:1335–1351.
- Stott, D., B. J. Francis, and R. B. Davies. 1996. *SABRE: a guide for users*. Version 3.1. Technical report. Centre for Applied Statistics, University of Lancaster, Lancaster.
- Sumida, B. H., A. I. Houston, J. M. McNamara, and W. D. Hamilton. 1990. Genetic algorithms and evolution. *Journal of Theoretical Biology* 147:59–84.
- van Baalen, J., and E. G. M. Prins. 1983. Growth and reproduction of *Digitalis purpurea* in different stages of succession. *Oecologia (Berlin)* 58:84–91.
- van der Meijden, E., and R. E. van de Waals-Kooi. 1979. The population ecology of *Senecio jacobaea* in a sand dune system. I. Reproductive strategy and the biennial habit. *Journal of Ecology* 67:131–153.
- Venables, W. N., and B. D. Ripley. 1997. *Modern applied statistics with S-PLUS*. Springer, New York.
- Weiner, J. 1982. A neighborhood model of annual-plant interference. *Ecology* 63:1237–1241.
- Werner, P. A. 1975. Predictions of fate from rosette size in teasel (*Dipsacus fullonum* L.). *Oecologia (Berlin)* 20: 197–201.
- Wesselingh, R. A., and T. J. de Jong. 1995. Bidirectional selection on threshold size for flowering in *Cynoglossum officinale* (hound's tongue). *Heredity* 74:415–424.
- Wesselingh, R. A., and P. G. L. Klinkhamer. 1996. Threshold size for vernalization in *Senecio jacobaea*: genetic variation and response to artificial selection. *Functional Ecology* 10:281–288.
- Wesselingh, R. A., T. J. de Jong, P. G. L. Klinkhamer, M. J. Vandijk, and E. G. M. Schlatmann. 1993. Geographical variation in threshold size for flowering in *Cynoglossum officinale*. *Acta Botanica Neerlandica* 42:81–91.
- Wesselingh, R. A., P. G. L. Klinkhamer, T. J. de Jong, and E. G. M. Schlatmann. 1994. A latitudinal cline in vernalization requirement in *Cirsium vulgare*. *Ecography* 17:272–277.
- Wesselingh, R. A., P. G. L. Klinkhamer, T. J. de Jong, and L. A. Boorman. 1997. Threshold size for flowering in different habitats: effects of size-dependent growth and survival. *Ecology* 78:2118–2132.
- Young, J. A., and R. A. Evans. 1972. Germination and persistence of achenes of Scotch thistle. *Weed Science* 20:98–101.
- Young, T. P. 1981. A general-model of comparative fecundity for semelparous and iteroparous life histories. *American Naturalist* 118:27–36.
- . 1984. The comparative demography of semelparous *Lobelia telekii* and iteroparous *Lobelia keniensis* on Mount Kenya. *Journal of Ecology* 72:637–650.
- . 1990. Evolution of semelparity in Mount Kenya lobelias. *Evolutionary Ecology* 4:157–171.
- Ziolkowski, M., and J. Kozłowski. 1983. Evolution of body size: an optimization model. *Mathematical Biosciences* 64: 127–143.